

Ab-initio methods for nuclei (part II)

Alessandro Lovato



Variational Monte Carlo

Remember that the numerator of the expectation value of the Hamiltonian for a system of A particles interacting with a spin-independent potential reads

$$E_T = \int dR \Psi_T^*(R) H \Psi_T(R) \quad R \equiv \mathbf{r}_1, \dots, \mathbf{r}_A$$

In order to use the central limit theorem, the former integral has to be rewritten as

$$E_T = \int dR |\Psi_T(R)|^2 E_L(R)$$

where we have defined the **local energy**

$$E_L(R) \equiv \frac{H \Psi_T(R)}{\Psi_T(R)}$$

Since it is positive and integrable, $|\Psi_T(R)|^2$ can be regarded as a probability density.

In order to compute the trial energy one has to find a way to sample $|\Psi_T(R)|^2$


M(RT)² algorithm

To begin with, consider a 1-D harmonic oscillator. We want to sample the probability distribution described by the modulus squared of our trial wave function

$$P(x) \equiv |\Psi_T(x)|^2 \qquad \Psi_T(x) = \exp\left(-\alpha \frac{x^2}{2}\right)$$

M(RT)² algorithm is based on the idea of random walk in the space of the random variable x . The game consists of generating a random variable applying a transformation to another. This “moving” point is called walker.

$$P_{i+1}(x_{i+1}) = \int dx_i P_i(x_i) T(x_i \rightarrow x_{i+1})$$

 **Transition probability**

By recursively applying the same transformation we get

$$P_n(x_n) = \int dx_1 \dots dx_{n-1} P_1(x_1) T(x_1 \rightarrow x_2) \dots T(x_{n-1} \rightarrow x_n)$$

Under some very general conditions it can be proven that

$\lim_{n \rightarrow \infty} P_n(x_n) = P(x) \Rightarrow$ where $P(x)$ only depends on T

M(RT)² algorithm

Let us impose a further condition, i.e. that the asymptotic distribution is an “equilibrium” state:

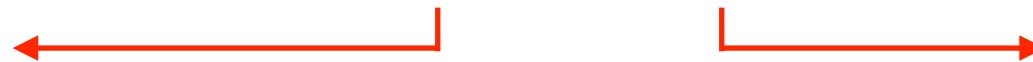
$$P(x)T(x \rightarrow y) = P(y)T(y \rightarrow x)$$

The latter is called detailed balance condition, because it does not hold only on average, but it tells that point by point there is no net flux of probability!

We can arbitrarily split the transition probability in two terms

$$T(x \rightarrow y) = G(x \rightarrow y)A(x \rightarrow y)$$

It describes the probability of moving the walker from $x \rightarrow y$.



It tells whether the proposed move is accepted or rejected.

The detailed balance then reads

$$\frac{A(y \rightarrow x)}{A(x \rightarrow y)} = \frac{P(x)G(x \rightarrow y)}{P(y)G(y \rightarrow x)}$$

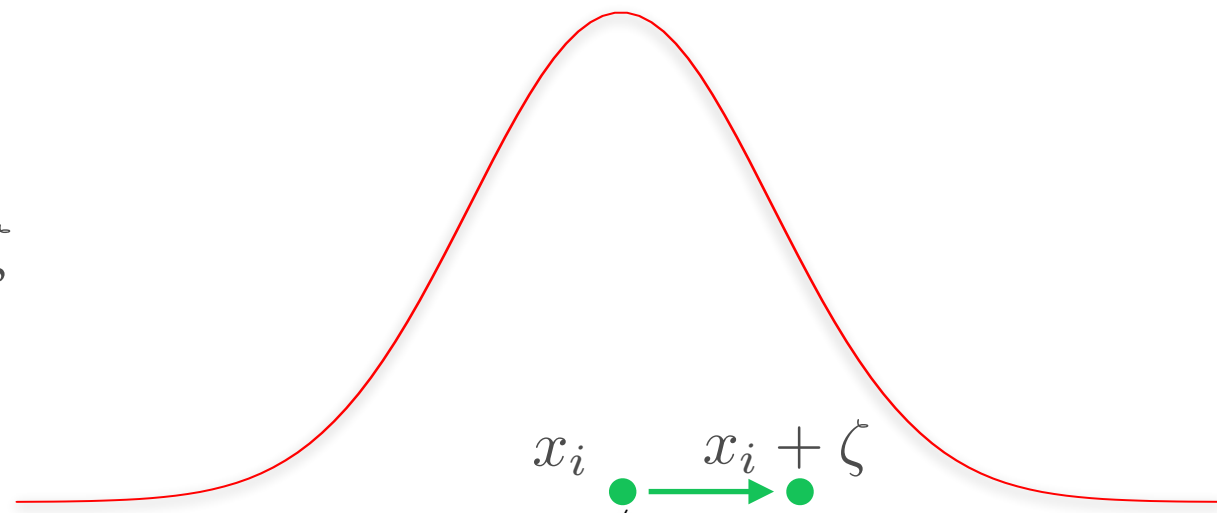
It can be easily checked that the following acceptance probability satisfies the above requirement

$$A(y \rightarrow x) = \min \left(1, \frac{P(x)G(x \rightarrow y)}{P(y)G(y \rightarrow x)} \right)$$

M(RT)² algorithm

In QMC we use a very simple prescription for $G(x \rightarrow y)$, which in 1-D corresponds to shifting a point by a value distributed according to a gaussian distribution

$$x_{i+1} = x_i + \zeta$$



In the many-particle case, the one dimensional gaussian is replaced by a three-dimensional one for each of the particles.

Since the probability of going from x to y is the same as the one for going from y to x , it turns out that

$$G(x \rightarrow y) = G(y \rightarrow x) \quad \longleftrightarrow \quad A(y \rightarrow x) = \min \left(1, \frac{P(x)}{P(y)} \right)$$

M(RT)² applied to VMC

At this point, we can describe the Metropolis algorithm for a VMC calculation in the 1-D case

Step 0 - Start from a “flat” distribution of walkers on the coordinate x

Step 1 - Move the walkers according to $G(x_i \rightarrow y_{i+1})$, i.e. $y_{i+1} = x_i + \zeta$

Step 2 - Compute the acceptance probability $A(x_i \rightarrow y_{i+1}) = \min \left(1, \frac{|\Psi_T(y_{i+1})|^2}{|\Psi_T(x_i)|^2} \right)$

Step 3 - Accept or reject the proposed move

$$\frac{|\Psi_T(y_{i+1})|^2}{|\Psi_T(x_i)|^2} > \xi \Rightarrow x_{i+1} = y_{i+1}$$

$$\frac{|\Psi_T(y_{i+1})|^2}{|\Psi_T(x_i)|^2} \leq \xi \Rightarrow x_{i+1} = x_i$$

Nuclear VMC wave function

A good trial wave function to describe a nucleus has to reflect the complexity of the nuclear potential

It contains 3-body correlations arising from the three-body potential

$$\Psi_T = \left[1 + \sum_{i < j < k} \tilde{U}_{ijk}^{\text{TNI}} \right] \Psi_P \longleftrightarrow \tilde{U}_{ijk} \equiv \tilde{\epsilon}_A V_{ijk}^A + \tilde{\epsilon}_R V_{ijk}^R$$

The pair correlated wave function is written in terms of operator correlations arising from the 2-body potential

$$\Psi_P = \left[\mathcal{S} \prod_{i < j} (1 + U_{ij}) \right] \Psi_J \longleftrightarrow U_{ij} = \sum_{p=2,6} u^p(r_{ij}) O_{ij}^p$$

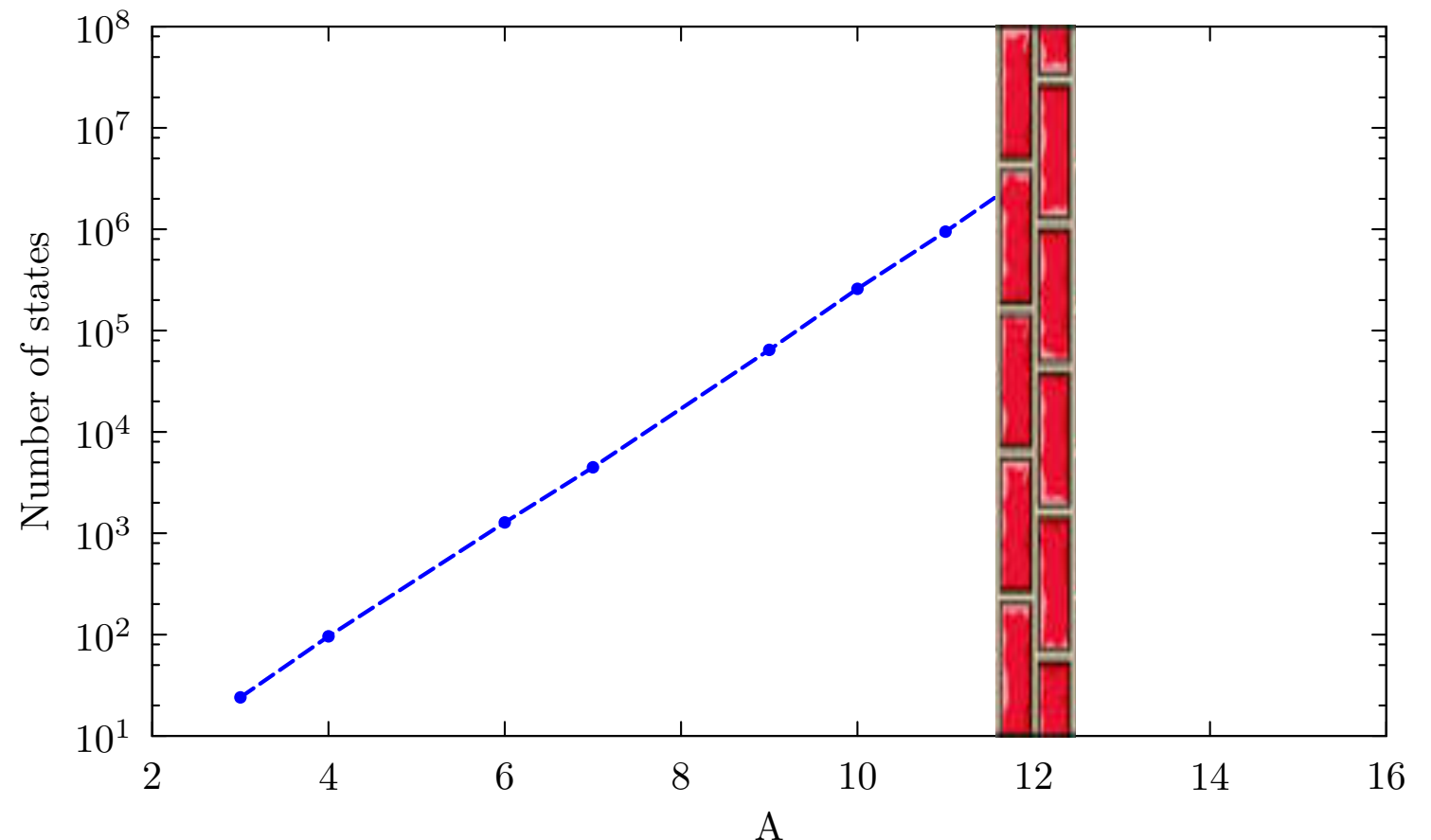
The total antisymmetric Jastrow wave function depends on the quantum numbers of the given nucleus

$$\Psi_J = \left[\prod_{i < j < k} f_{ijk}^c \right] \left[\prod_{i < j} f_{ij}^c \right] \Phi_A(J, M, T, T_3)$$

Spin-isospin degrees of freedom

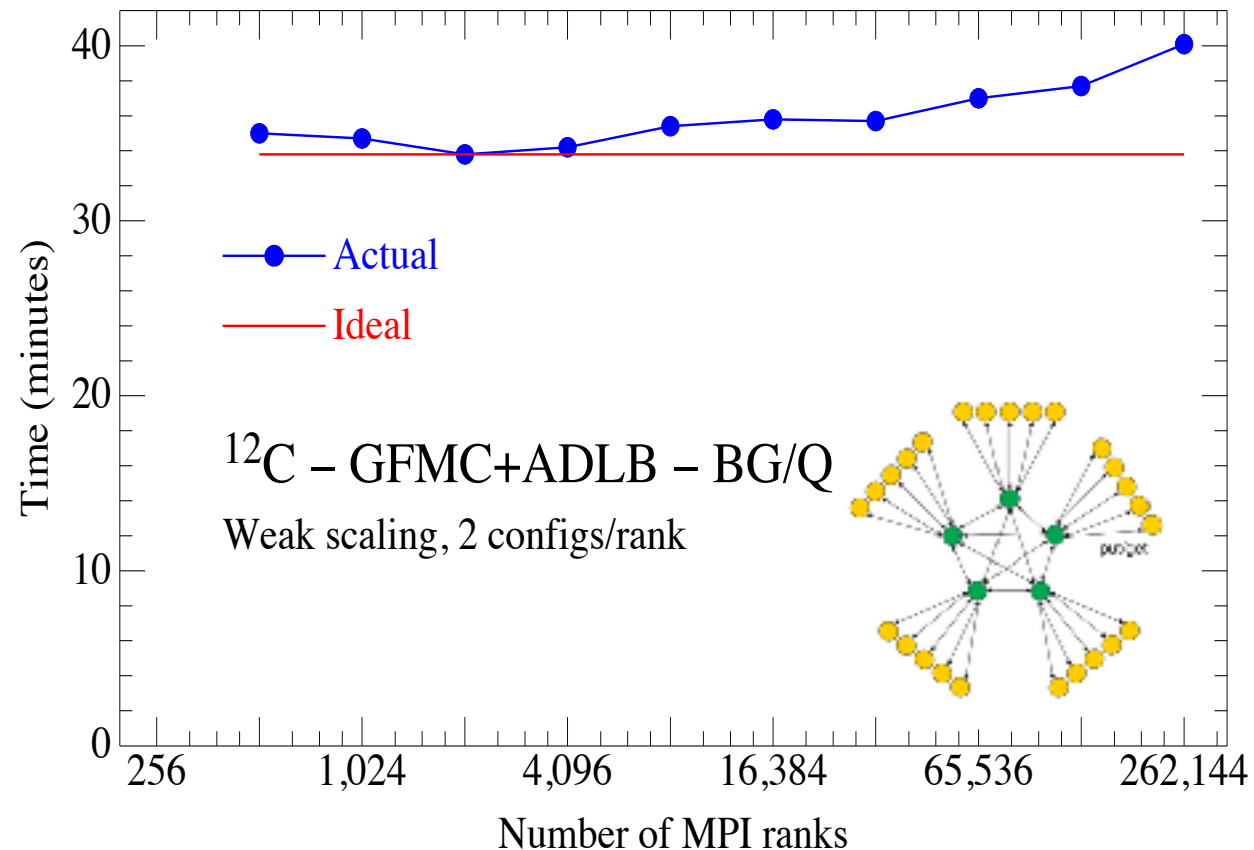
- A walker associated with wave function of the nucleus, do not only describes the positions of the protons and neutrons, but also their spin and isospin!
- The GFMC wave function is written as a complex vector, the coordinates of which represent a spin-isospin state of the system
- The ${}^3\text{H}$ case fits in the slide: the number of states grows exponentially with the number of nucleons

$$|\Psi_{3H}\rangle = \begin{pmatrix} a_{\uparrow\uparrow\uparrow} \\ a_{\uparrow\uparrow\downarrow} \\ a_{\uparrow\downarrow\uparrow} \\ a_{\uparrow\downarrow\downarrow} \\ a_{\downarrow\uparrow\uparrow} \\ a_{\downarrow\uparrow\downarrow} \\ a_{\downarrow\downarrow\uparrow} \\ a_{\downarrow\downarrow\downarrow} \end{pmatrix} \otimes \begin{pmatrix} a_{pnn} \\ a_{npn} \\ a_{nnp} \end{pmatrix}$$



Quantum Monte Carlo

- Joint efforts between physicists and computing scientists have proven to be essential for most of the recent advances nuclear theory
- GFMC has steadily undergone development to take advantage of each new generation of parallel machine and was one of the first to deliver new scientific results each time.



Diffusion Monte Carlo

- The accuracy of a VMC calculation is limited by the knowledge of the trial wave function.
- The **diffusion Monte Carlo (DMC)** method, overcomes this limitation by using a projection technique to enhance the true ground-state component of a starting trial wave function.
- The method relies on the observation that the trial wave function can be expanded in the complete set of eigenstates of the the hamiltonian according to

$$|\Psi_T\rangle = \sum_n c_n |\Psi_n\rangle \qquad H|\Psi_n\rangle = E_n |\Psi_n\rangle$$

which implies

$$\lim_{\tau \rightarrow \infty} e^{-(H-E_0)\tau} |\Psi_T\rangle = \lim_{\tau \rightarrow \infty} \sum_n c_n e^{-(E_n-E_0)\tau} |\Psi_n\rangle = c_0 |\Psi_0\rangle$$

where τ is the imaginary time. Hence, DMC projects out the exact lowest-energy state, provided the trial wave function it is not orthogonal to the ground state.

Diffusion Monte Carlo

- The direct calculation of $e^{-(H-E_0)\tau}$ for strongly-interacting systems involves prohibitive difficulties
- To circumvent this problem, the imaginary-time evolution is broken into N small imaginary-time steps, and complete sets of states are inserted

$$e^{-(H-E_0)\tau}|\Psi_T\rangle = \int dR_1 \dots dR_N |R_N\rangle \langle R_N| e^{-(H-E_0)\Delta\tau} |R_{N-1}\rangle \dots \\ \dots \langle R_2| e^{-(H-E_0)\Delta\tau} |R_1\rangle \Psi_T(R_1)$$

Note the analogy with the Feynman's path integrals in quantum and statistical mechanics !!!

- At imaginary-time $\tau_{i+1} = (i+1)\Delta\tau$ the walkers are distributed according to

$$\Psi(\tau_{i+1}, R_{i+1}) = \int dR_i \langle R_{i+1}| e^{(H-E_0)\Delta\tau} |R_i\rangle \Psi(\tau_i, R_i)$$

Diffusion Monte Carlo

The problem is then reduced to computing the **short-time Green's function** of the system

$$G(R_i \rightarrow R_{i+1}, \Delta\tau) = \langle R_i | e^{-(H-E_0)\Delta\tau} | R_{i+1} \rangle$$

The analytic solution of Green's function of the full hamiltonian is in general not known. An approximation to the Green's function can be obtained using the **Trotter-Suzuki formula**

$$\langle R_i | e^{-(T+V-E_0)\Delta\tau} | R_{i+1} \rangle = e^{E_0\Delta\tau} \langle R_i | e^{-T\Delta\tau} e^{-V\Delta\tau} | R_{i+1} \rangle + \mathcal{O}(\Delta\tau^2)$$

In the limit of small time-step, the Green's function factorizes

$$G(R_i \rightarrow R_{i+1}, \Delta\tau) \simeq G_d(R_i \rightarrow R_{i+1}, \Delta\tau) G_b(R_i \rightarrow R_{i+1}, \Delta\tau)$$

More accurate ways of factorizing the propagator have been derived

$$\langle R_i | e^{-(T+V-E_0)\Delta\tau} | R_{i+1} \rangle = e^{E_0\Delta\tau} \langle R_i | e^{-V/2\Delta\tau} e^{-T\Delta\tau} e^{-V/2\Delta\tau} | R_{i+1} \rangle + \mathcal{O}(\Delta\tau^3)$$

Diffusion Monte Carlo

The **free Green's function** satisfies the master equation of a diffusion stochastic process

$$-\frac{\partial}{\partial \tau} G_d(R_i \rightarrow R_{i+1}, \Delta \tau) = -\frac{\hbar^2}{2m} \nabla^2 G_d(R_i \rightarrow R_{i+1}, \Delta \tau)$$

It is given by a 3A-dimensional Gaussian describing the Brownian diffusion of A particles with a dynamic governed by random collisions

$$G_d(R_i \rightarrow R_{i+1}, \Delta \tau) = \left(\frac{m}{2\pi \hbar^2 \Delta \tau} \right)^{\frac{3A}{2}} e^{-\frac{m}{2\hbar^2 \Delta \tau} (R_i - R_{i+1})^2}$$

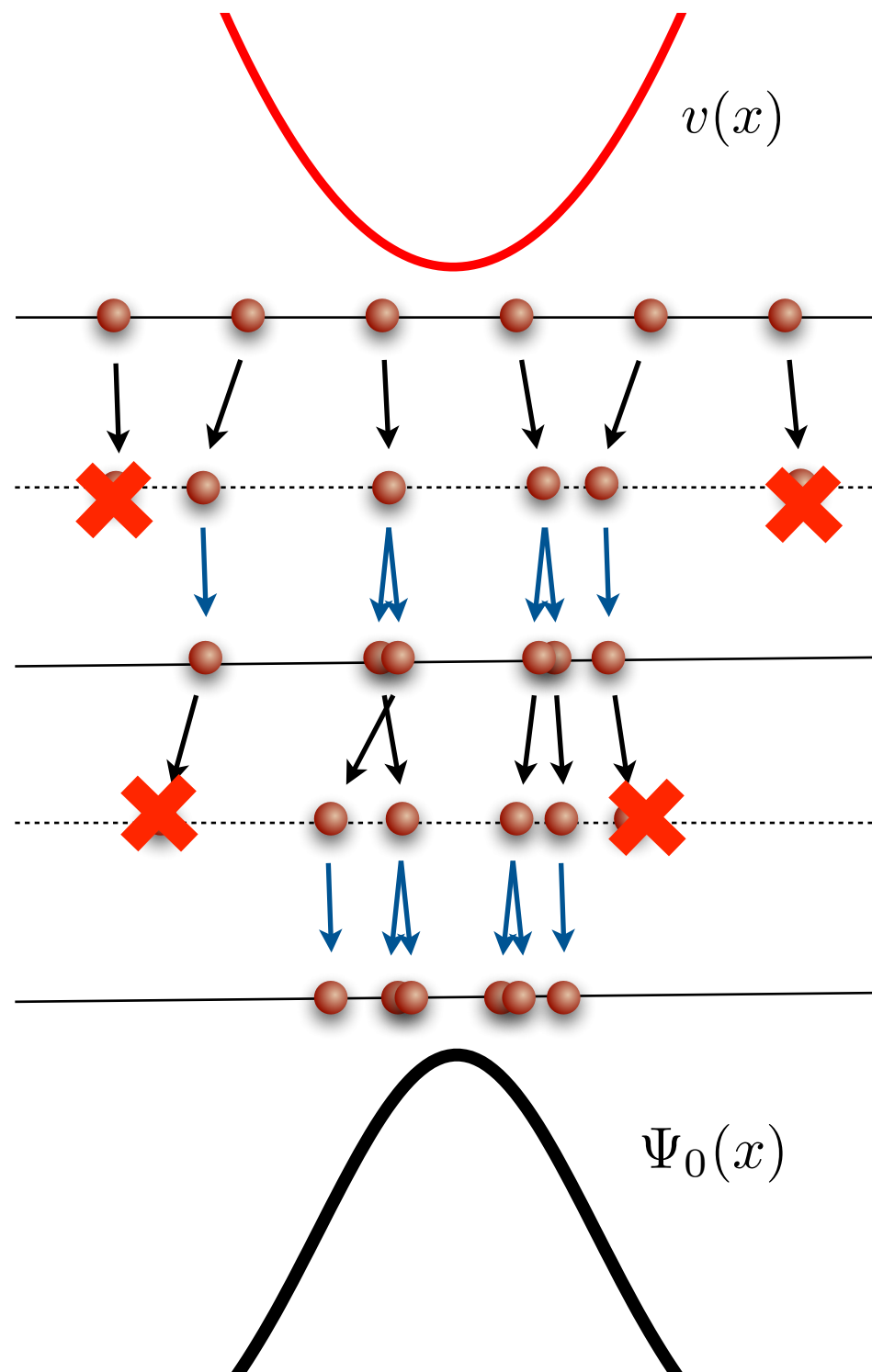
The **branching Green's function**, on the other hand, is simply given by

$$G_b(R_i \rightarrow R_{i+1}, \Delta \tau) = e^{-[V(R_{i+1}) - E_0] \Delta \tau}$$

Hence, at the imaginary time $\tau_{i+1} = (i+1)\Delta \tau$ the walkers are distributed according to

$$\Psi(\tau_{i+1}, R_{i+1}) = \left(\frac{m}{2\pi \hbar^2 \Delta \tau} \right)^{\frac{3A}{2}} \int dR_i e^{-\frac{m}{2\hbar^2 \Delta \tau} (R_i - R_{i+1})^2} e^{-[V(R_{i+1}) - E_0] \Delta \tau} \Psi(\tau_i, R_i)$$

Diffusion Monte Carlo



- A set of walkers is sampled from the trial wave function

- Gaussian drift for the kinetic energy

$$\left(\frac{m}{2\pi\hbar^2\Delta\tau} \right)^{\frac{1}{2}} e^{-\frac{m}{2\hbar^2\Delta\tau}(x_i - x_{i+1})^2}$$

- Branching and killing of the walkers induced by the potential weight

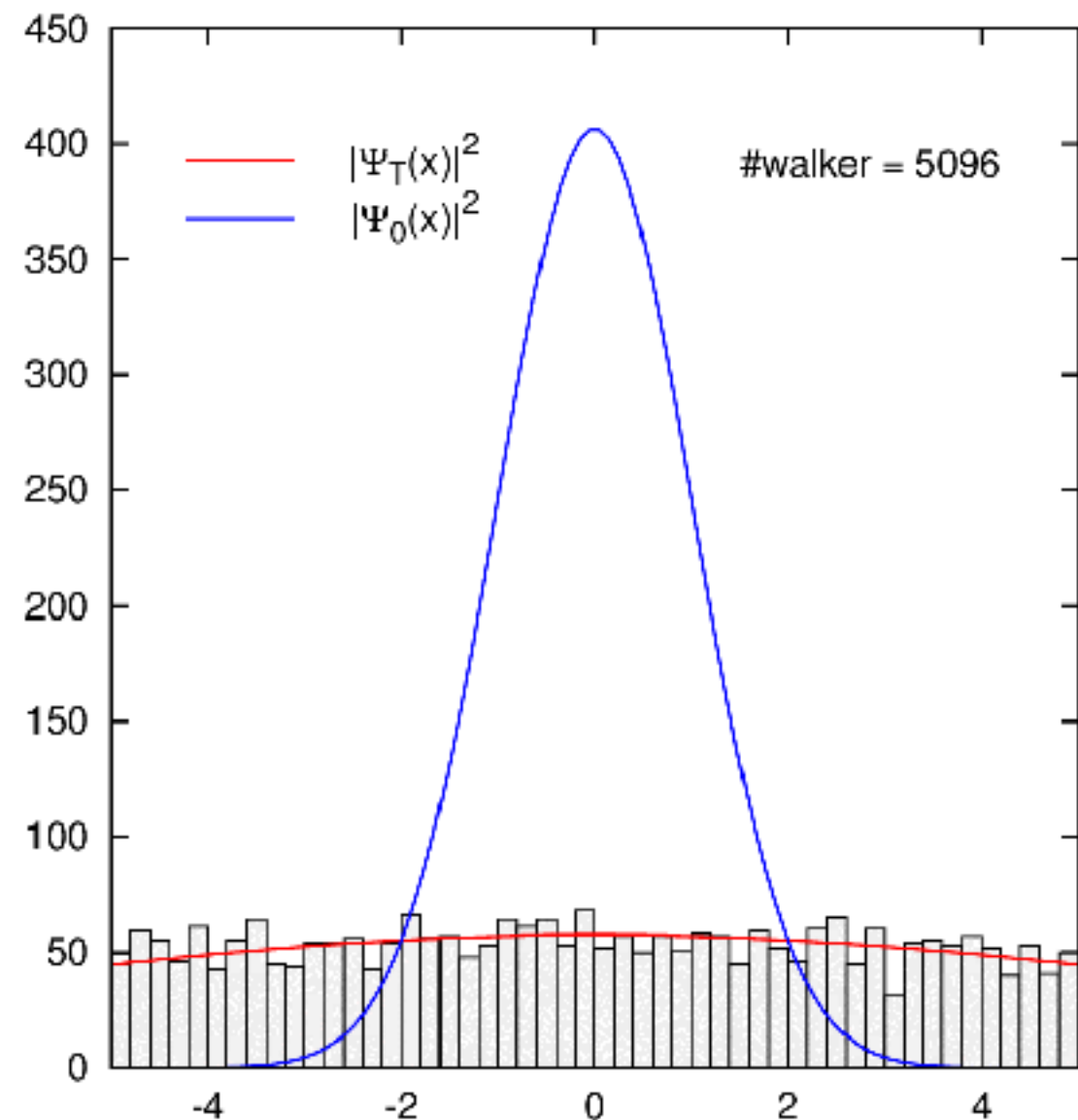
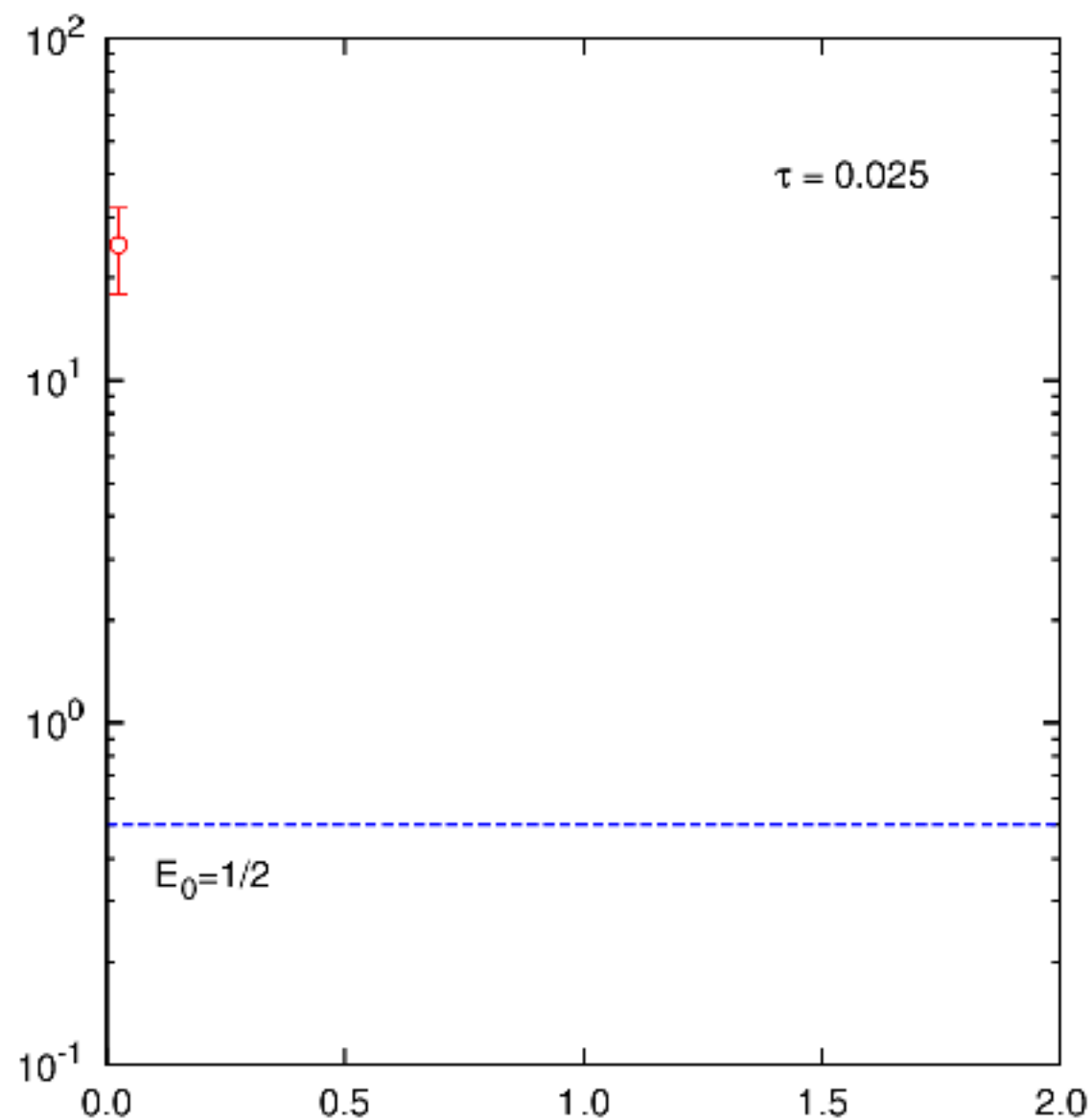
$$w(x_{i+1}) = e^{-[V(x_{i+1}) - E_0]\Delta\tau}$$

- Ground-state expectation values are estimated during the diffusion

$$\langle H \rangle = \frac{\sum_{x_i} \langle x_i | H | \Psi_T \rangle w(x_i)}{\sum_{x_i} \langle x_i | \Psi_T \rangle w(x_i)}$$

DMC for the 1d harmonic oscillator

$$H = -\frac{1}{2} \frac{d^2}{dx^2} + \frac{x^2}{2} \longleftrightarrow \begin{aligned} \Psi_0(x) &= e^{-x^2/2} \\ E_0 &= 1/2 \end{aligned}$$



Importance sampling

The algorithm as it was shown so far is not suitable for potentials presenting a divergent behavior

- A strongly repulsive potential (e.g. repulsive Coulomb, Lennard-Jones, Argonne v_{18}) will result in a very fast absorption of walkers, eventually killing the whole population.
- An attractive potential (e.g. Coulomb attraction between the nucleus and electrons in an atom) will generate an exponentially growing population

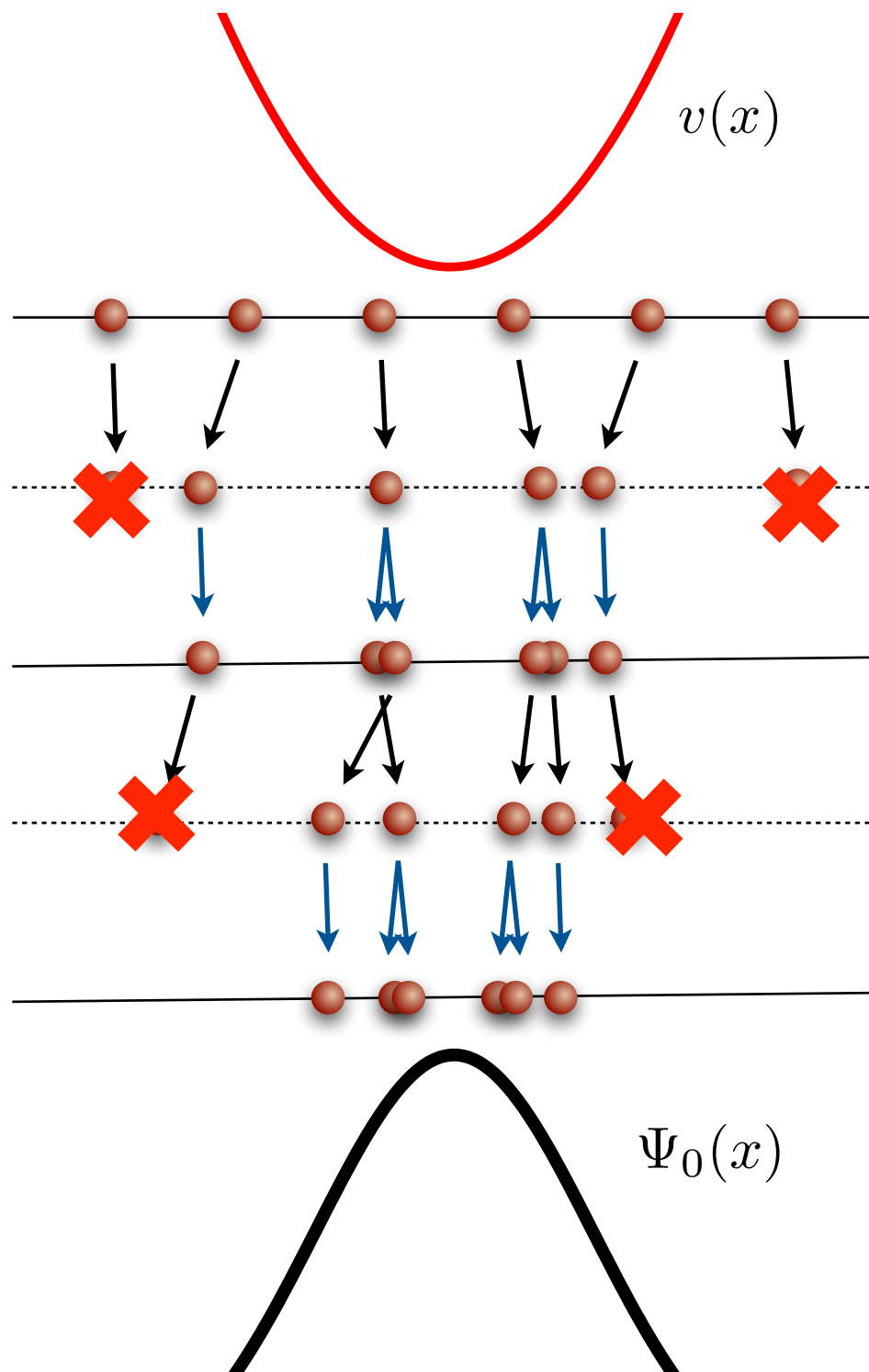
The idea of the importance sampling technique consists in using the knowledge of the trial wave function to guide the imaginary-time projection. Consider

$$f(\tau_i, R_i) \equiv \Psi_T(R_i)\Psi(\tau_i, R_i)$$

Its imaginary-time evolution is given by

$$f(\tau_{i+1}, R_{i+1}) = \int dR_i G_d(R_i \rightarrow R_{i+1}, \Delta\tau) G_b(R_i \rightarrow R_{i+1}, \Delta\tau) \frac{\Psi_T(R_{i+1})}{\Psi_T(R_i)} f(\tau_i, R_i)$$

Importance sampling diffusion Monte Carlo



- A set of walkers is sampled from the trial wave function

- Gaussian drift for the kinetic energy

$$\left(\frac{m}{2\pi\hbar^2\Delta\tau} \right)^{\frac{1}{2}} e^{-\frac{m}{2\hbar^2\Delta\tau}(x_i - x_{i+1})^2}$$

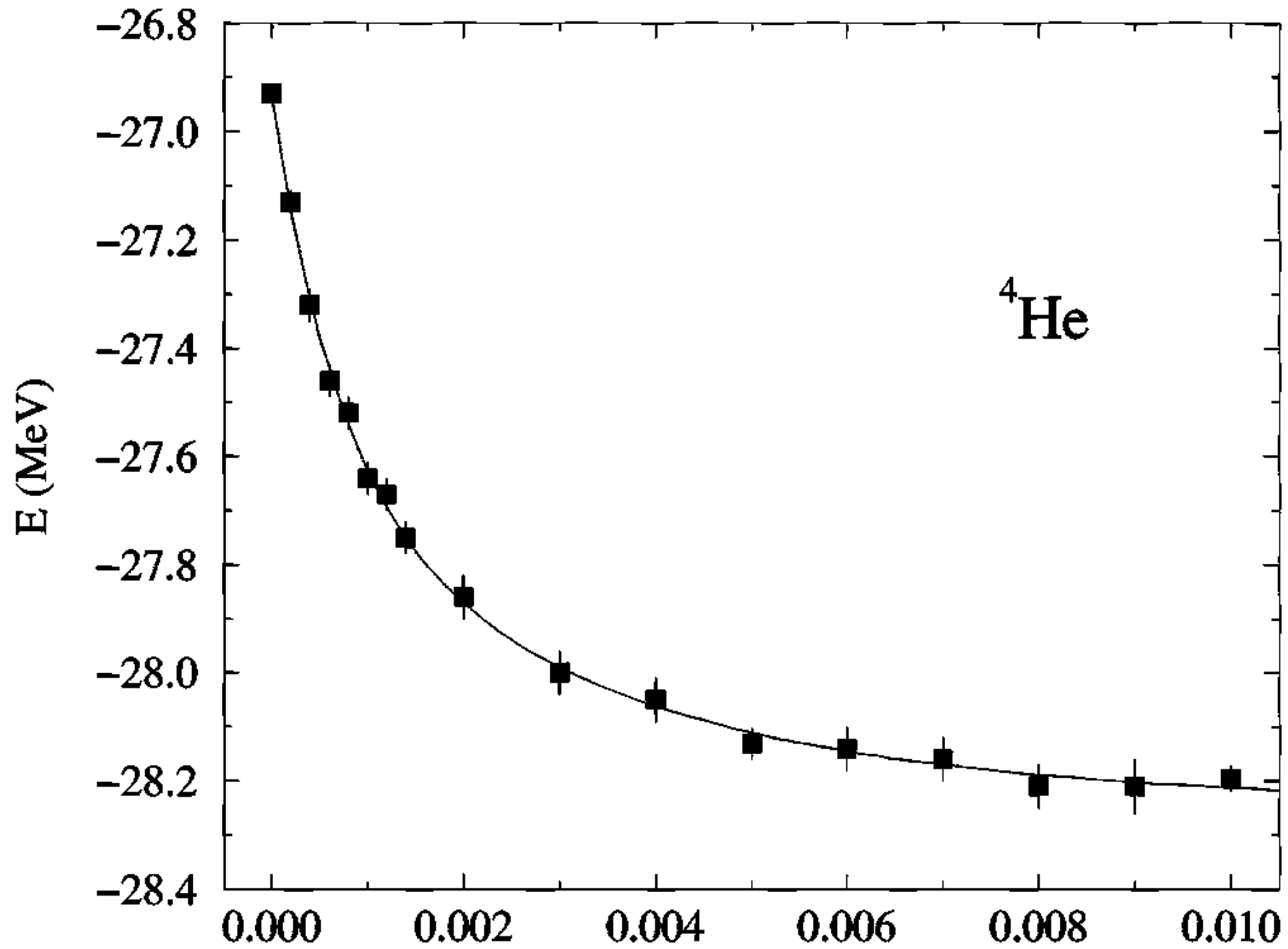
- Branching and killing of the walkers induced by the potential weight

$$w(x_i) = e^{-[V(x_{i+1}) - E_0]\Delta\tau} \frac{\Psi_T(x_{i+1})}{\Psi_T(x_i)}$$

- Ground-state expectation values are estimated during the diffusion

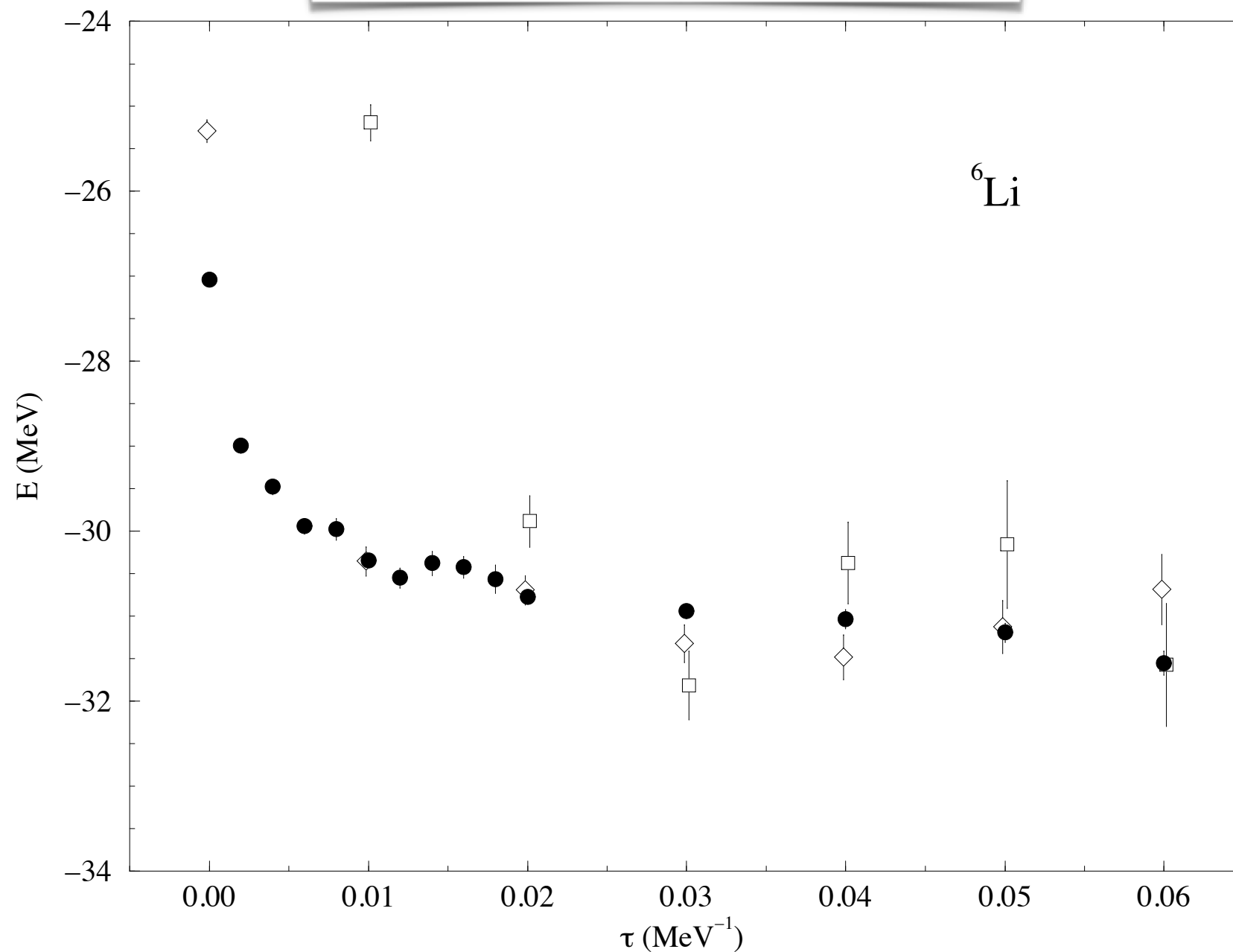
$$\langle H \rangle = \frac{\sum_{x_i} \frac{\langle x_i | H | \Psi_T \rangle}{\langle x_i | \Psi_T \rangle} w(x_i)}{\sum_{x_i} w(x_i)}$$

Imaginary-time evolution



Imaginary-time evolution

B. S. Pudliner et al. PRC 56 1720 (1995)



Solid circles: the full trial wave functions

Open diamonds: no three-body correlations

Open squares: no three-body correlations no tensor correlations

One slide on the sign problem

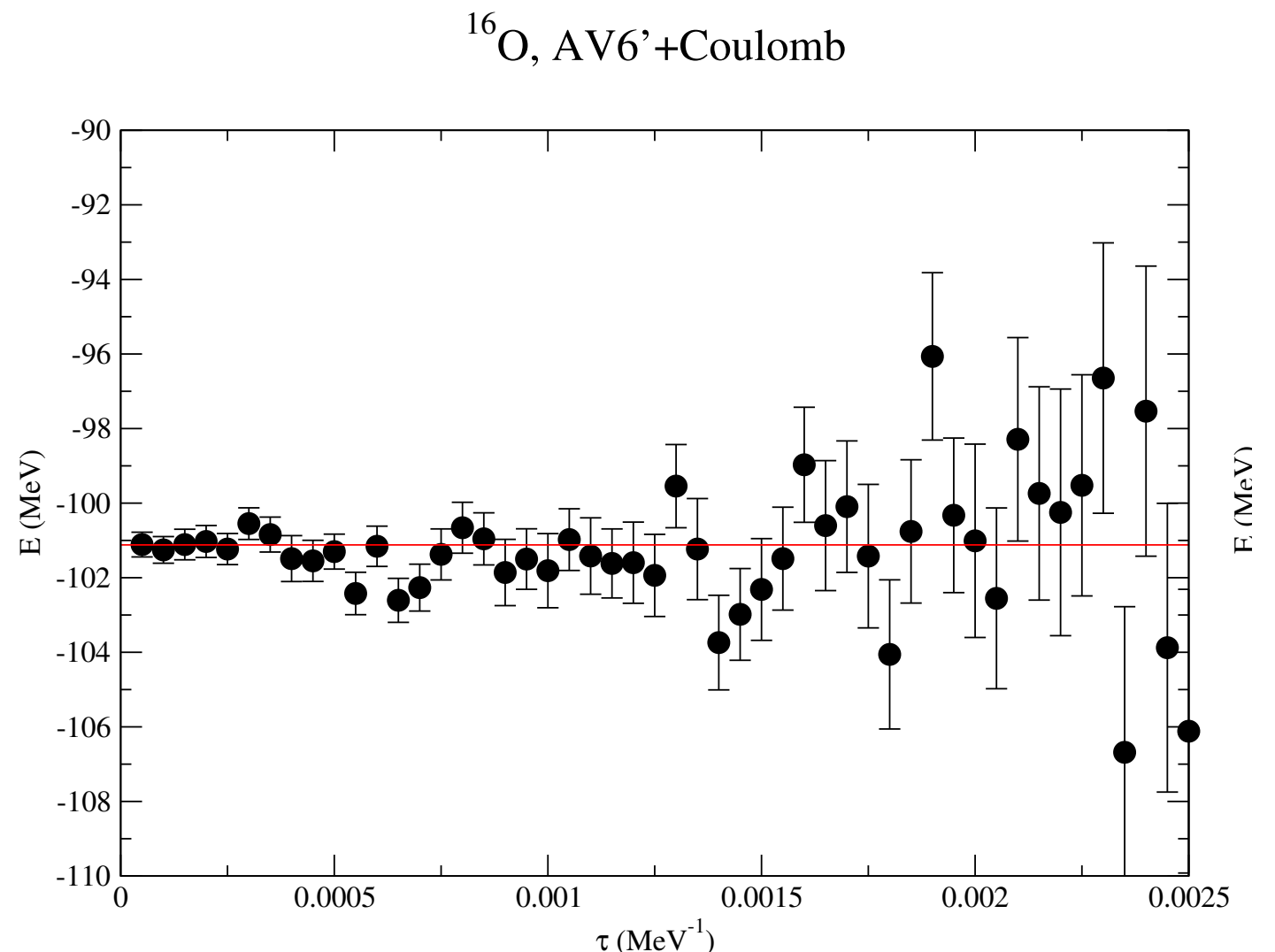
So far we have implicitly assumed that the wave function can be given a probabilistic interpretation, **but** a fermionic wave function is NOT positive definite. In the nuclear case it is not even real!

Since the ground-state of a given Hamiltonian is always bosonic, searching for the ground-state energy of a fermionic system is very similar to projecting onto an excited state.

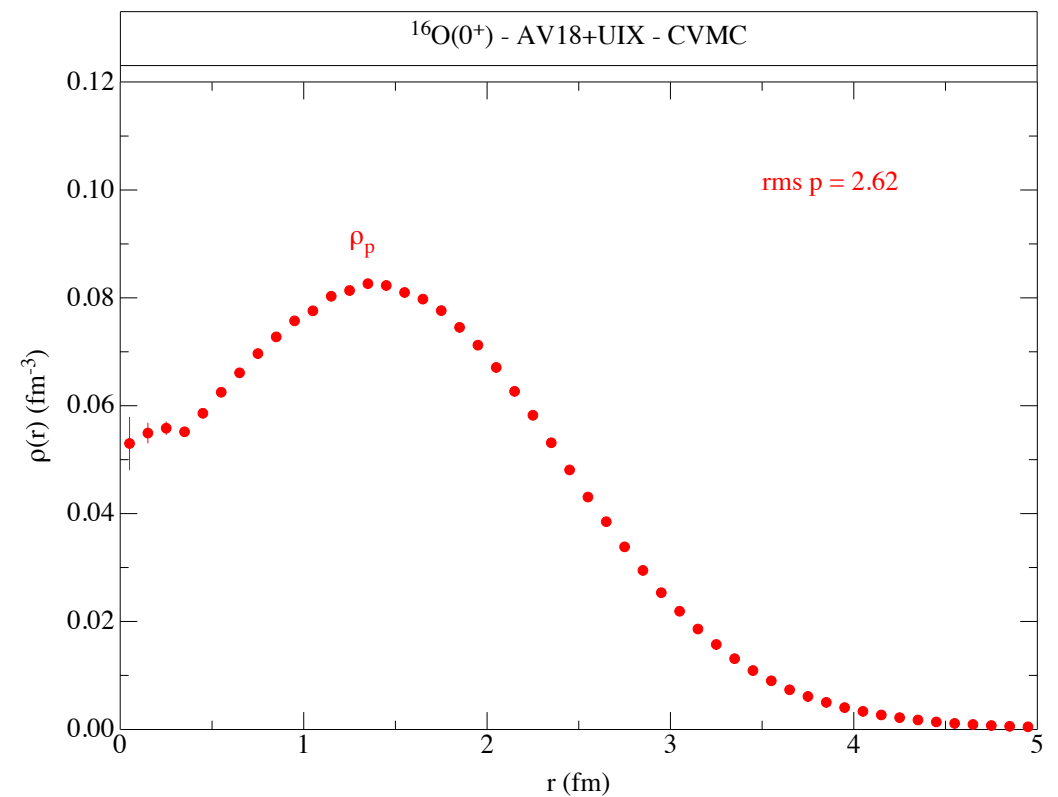
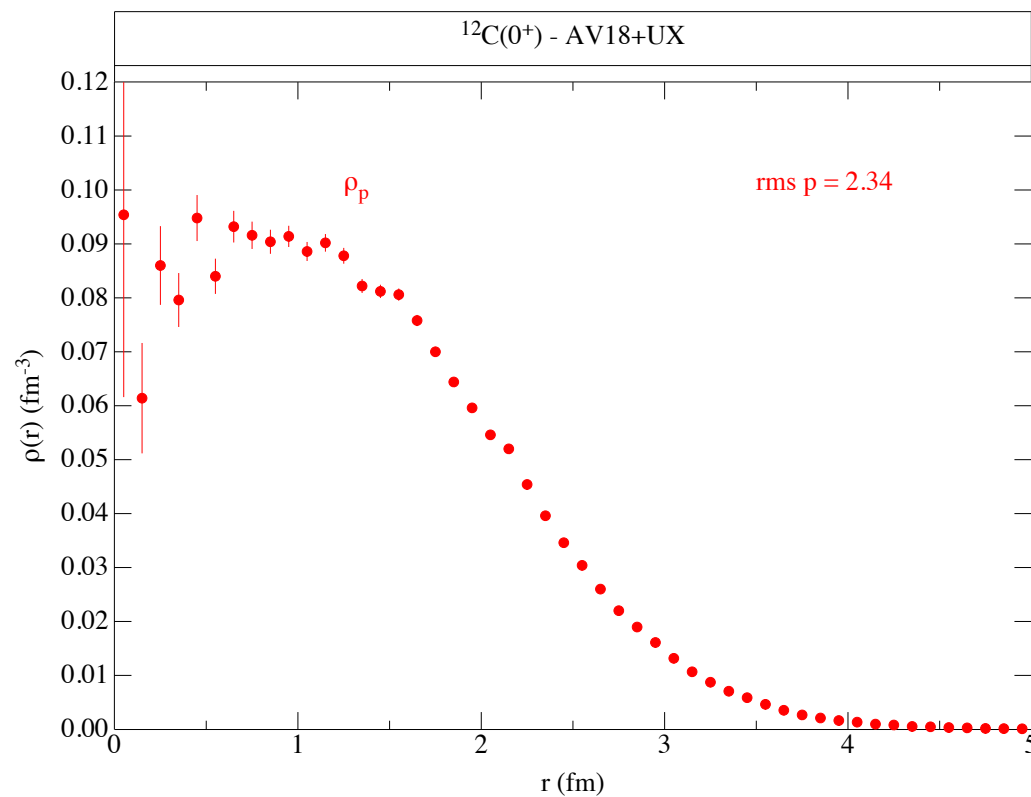
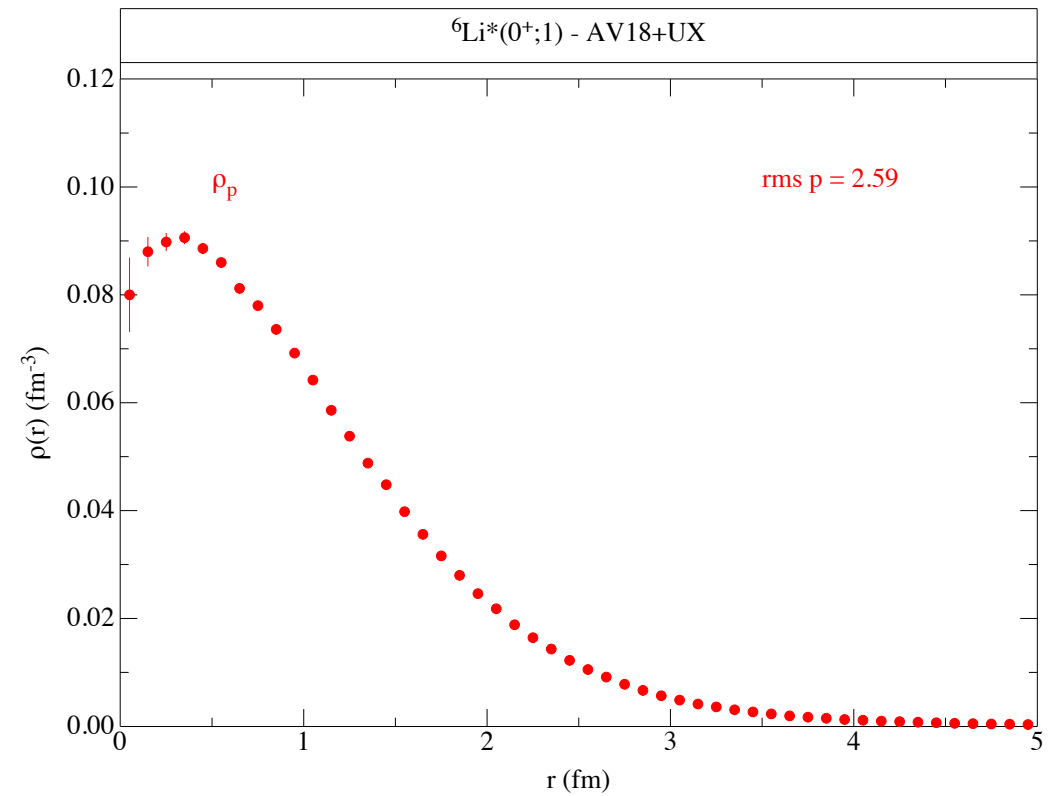
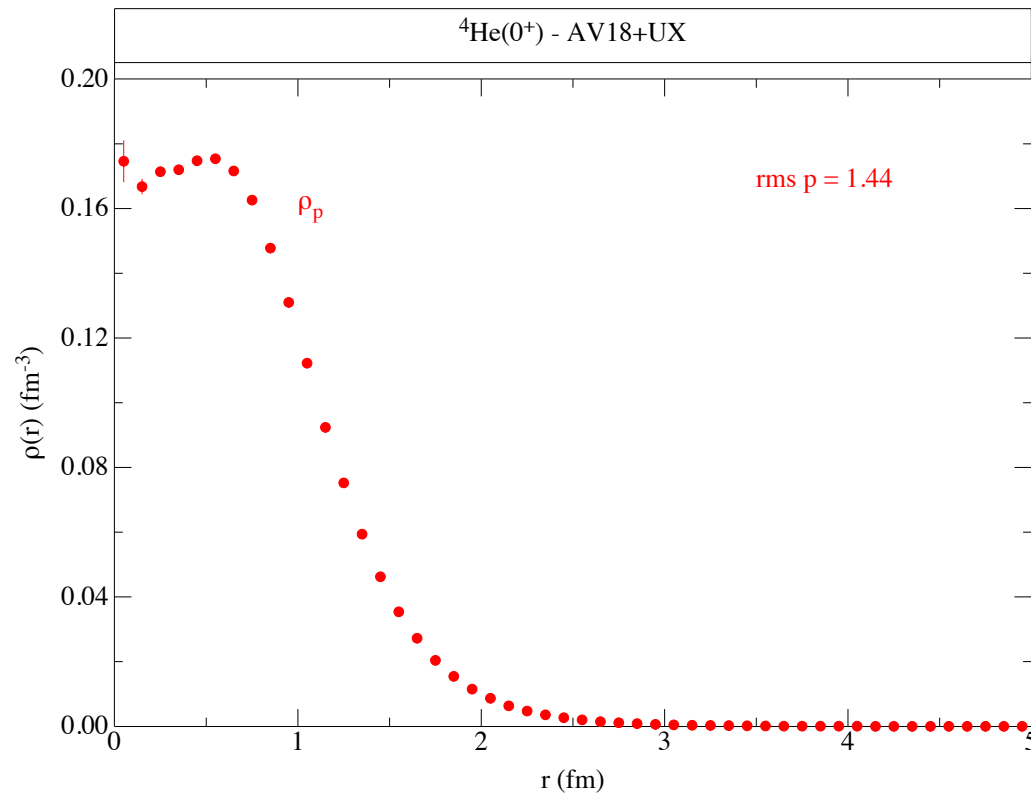
since the trial wave function is fermionic, the energy converges to exact eigenvalue with an exponentially growing statistical error. In other words, the signal to noise ratio decays exponentially.

This issue, known as **sign problem**, is common to all Monte Carlo approaches when applied to fermionic system

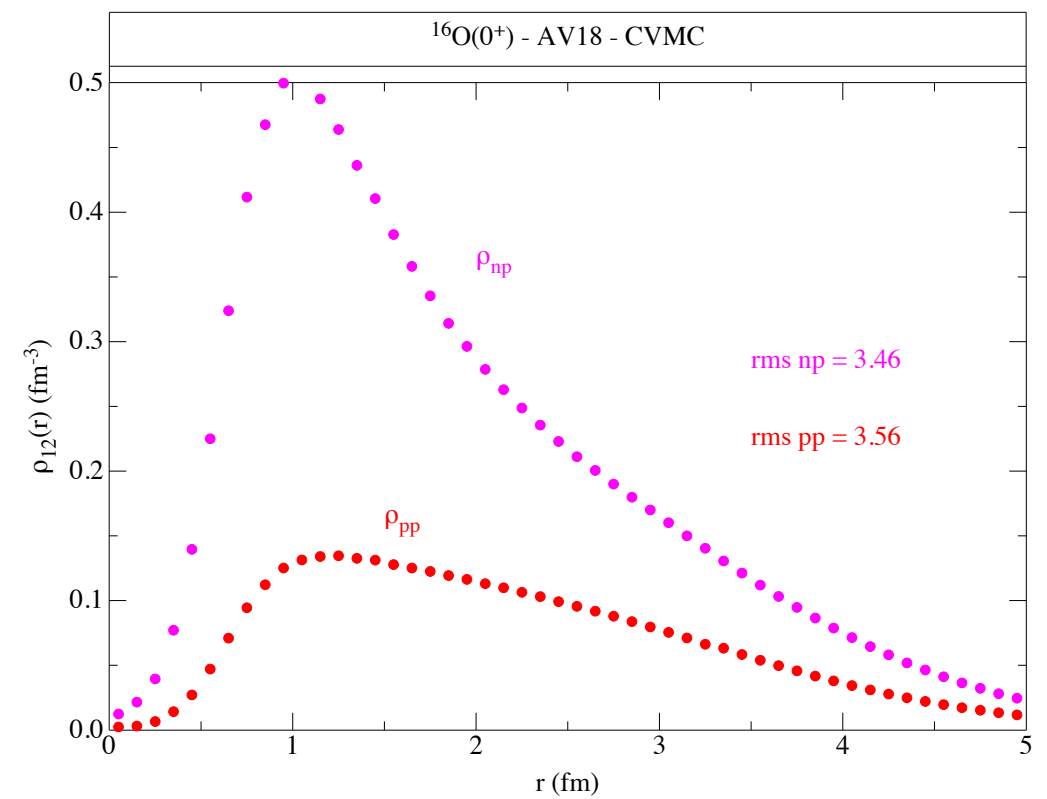
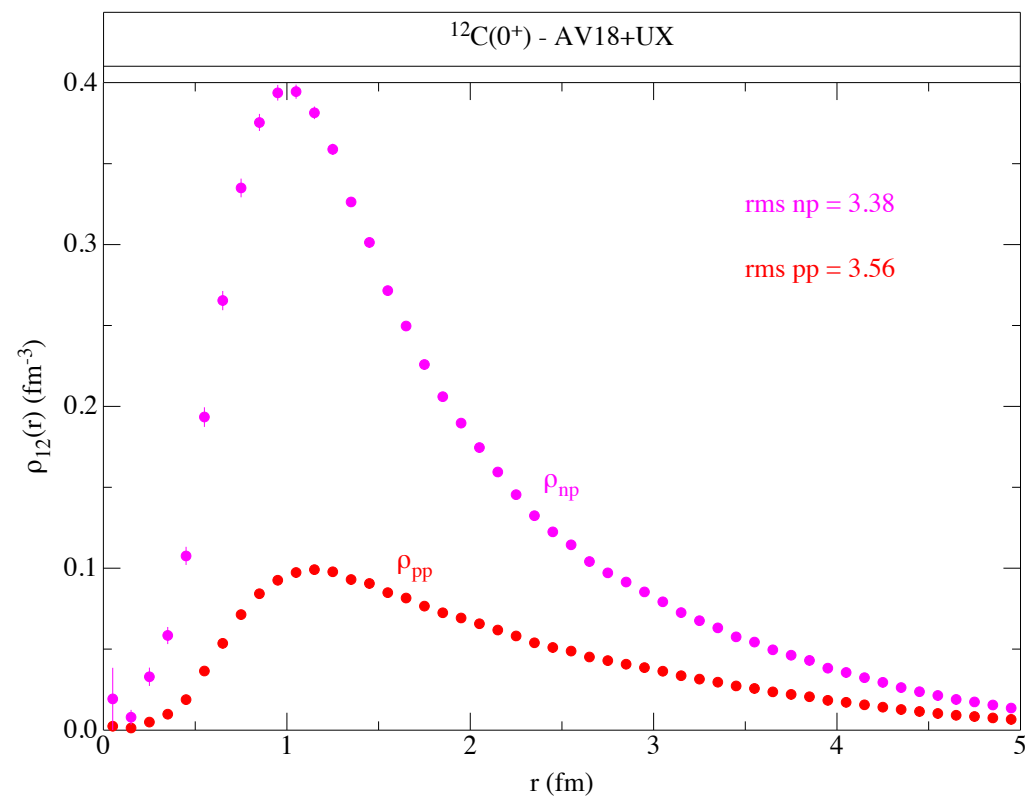
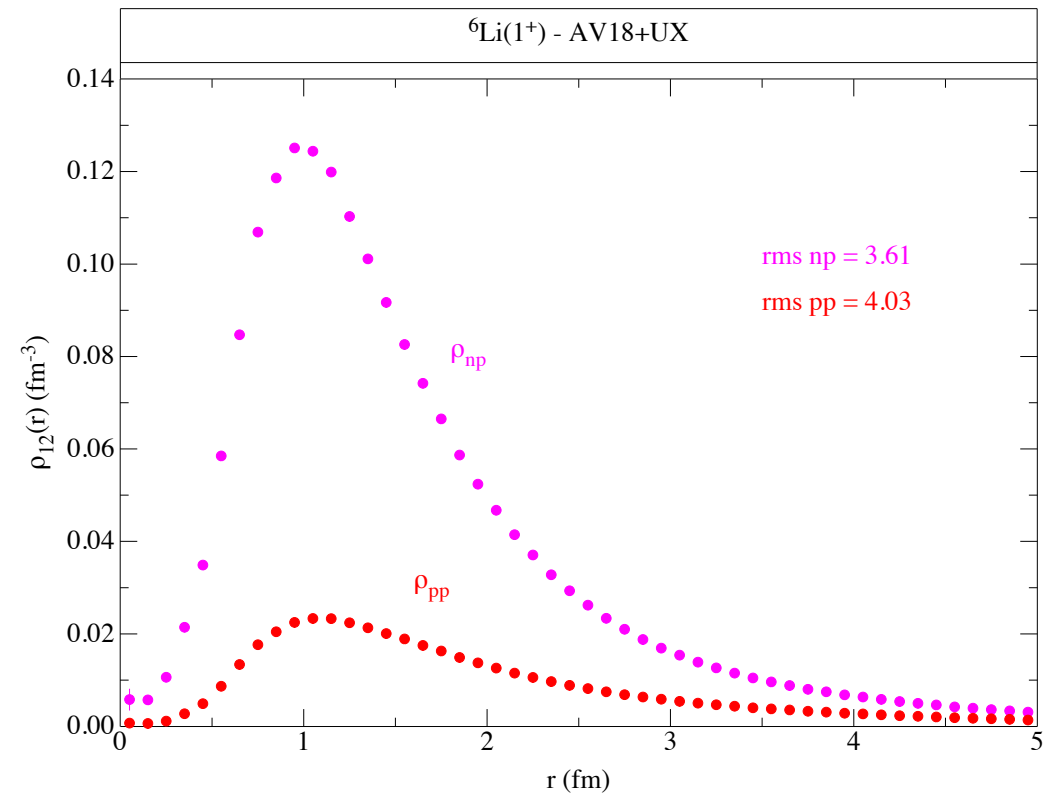
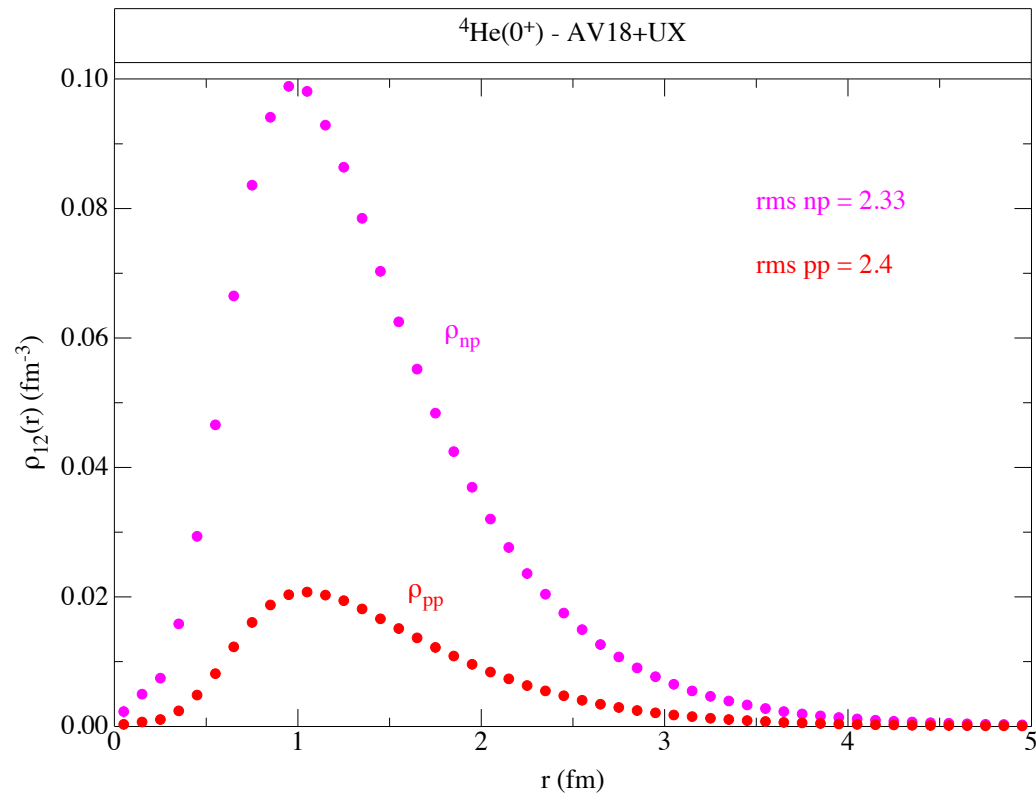
Many workarounds: fixed node, constrained path... but no definitive solution so far.



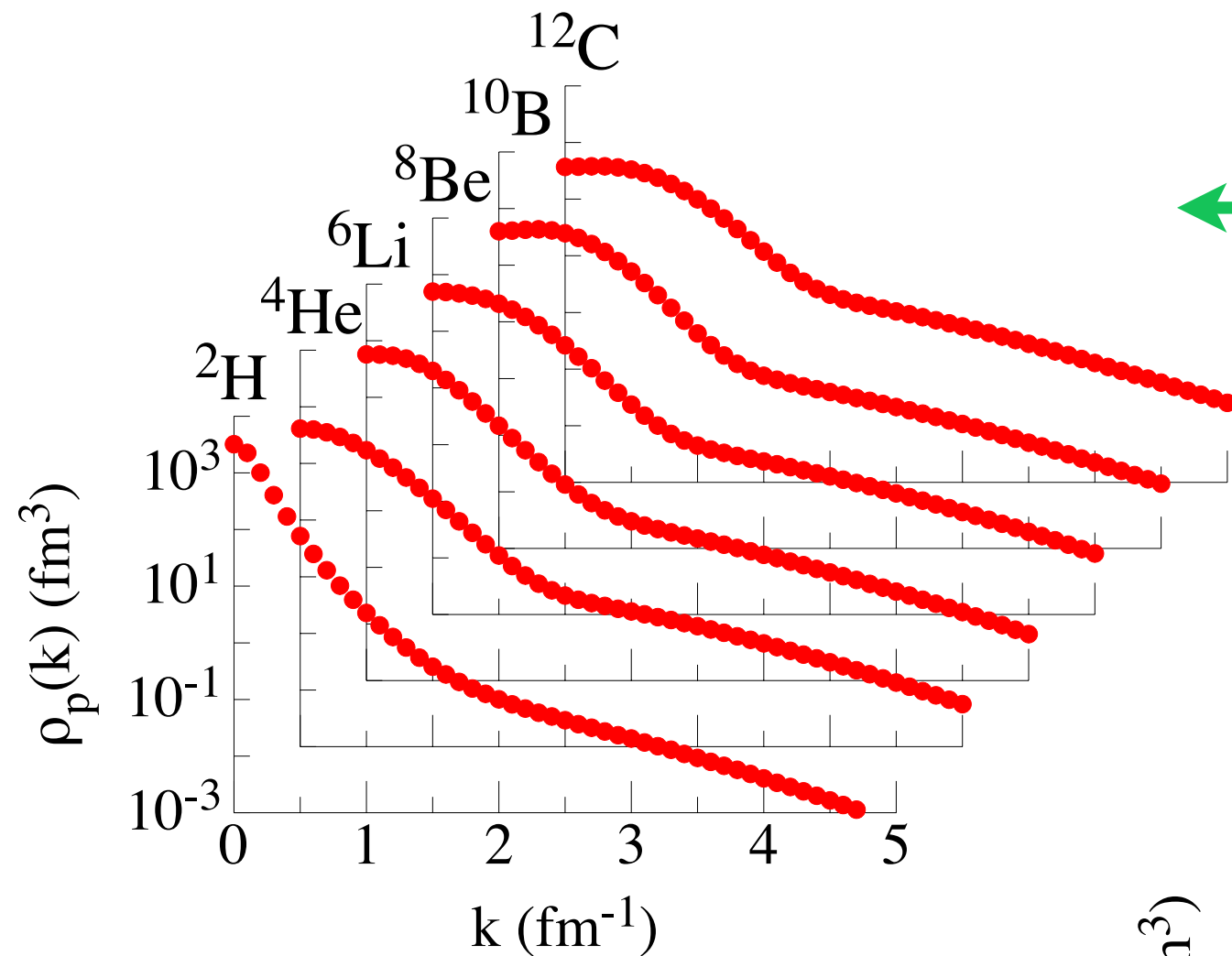
Single-nucleon densities



Two-nucleon densities

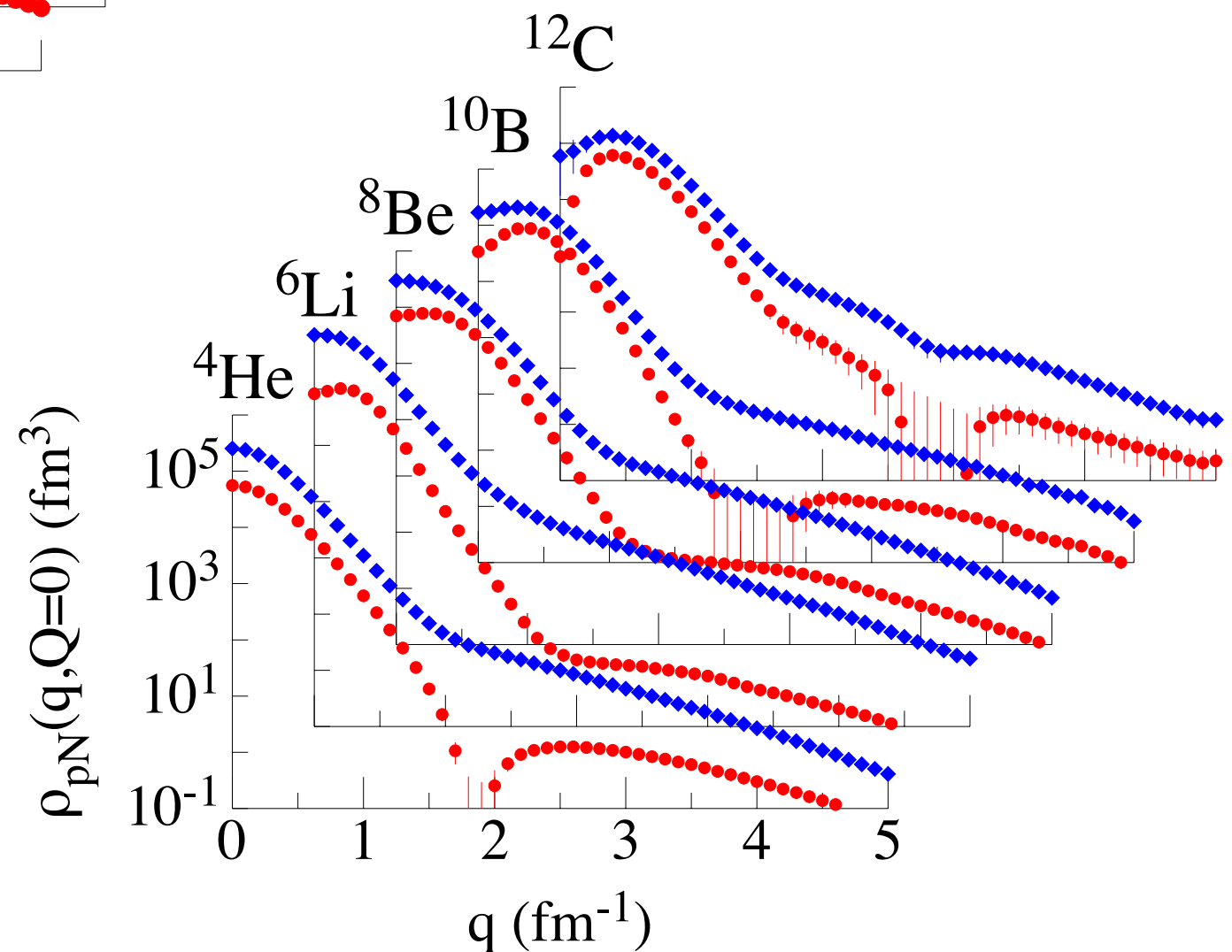


Momentum distributions



← Single-nucleon momentum distribution

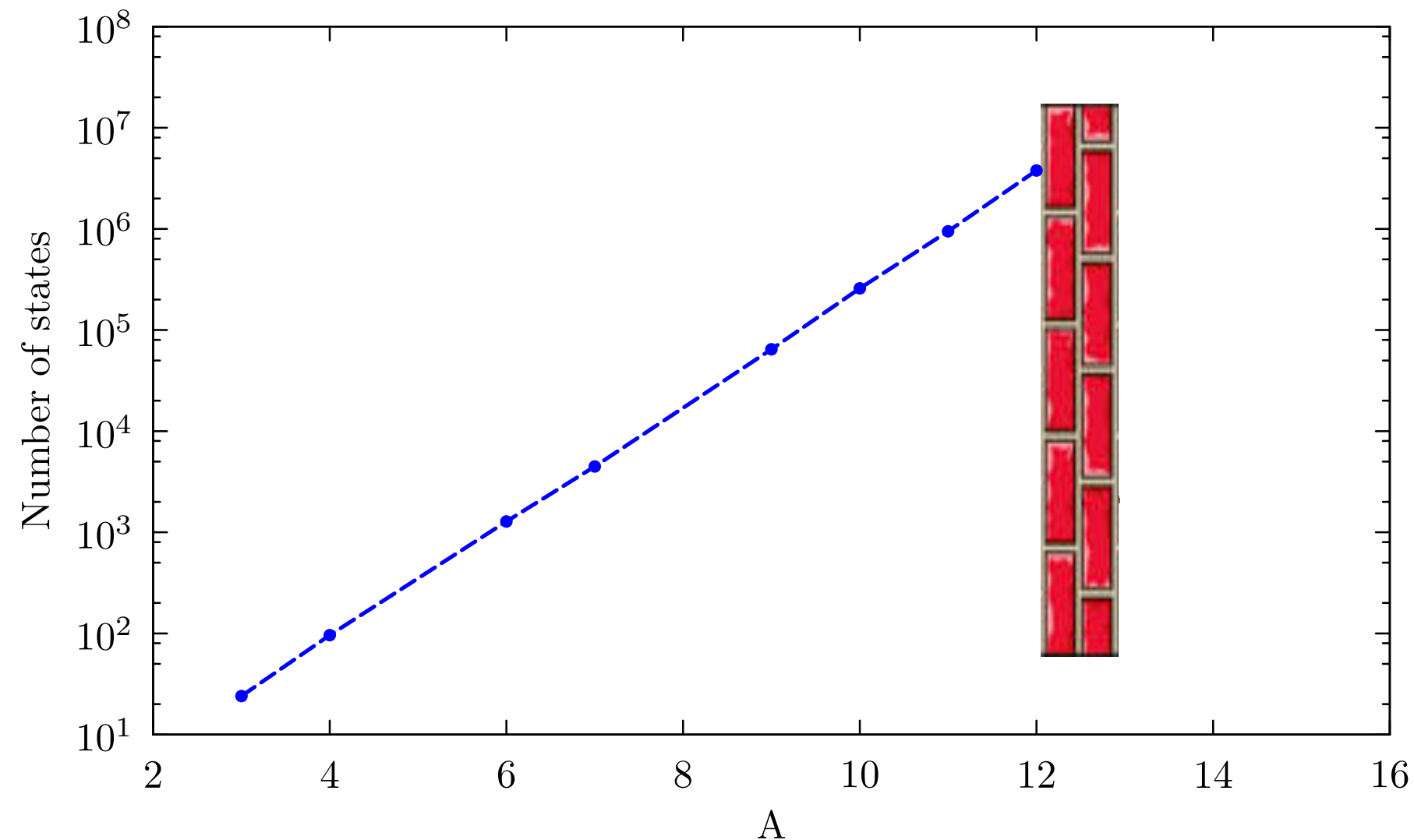
Two-nucleon momentum distribution →



Quantum Monte Carlo

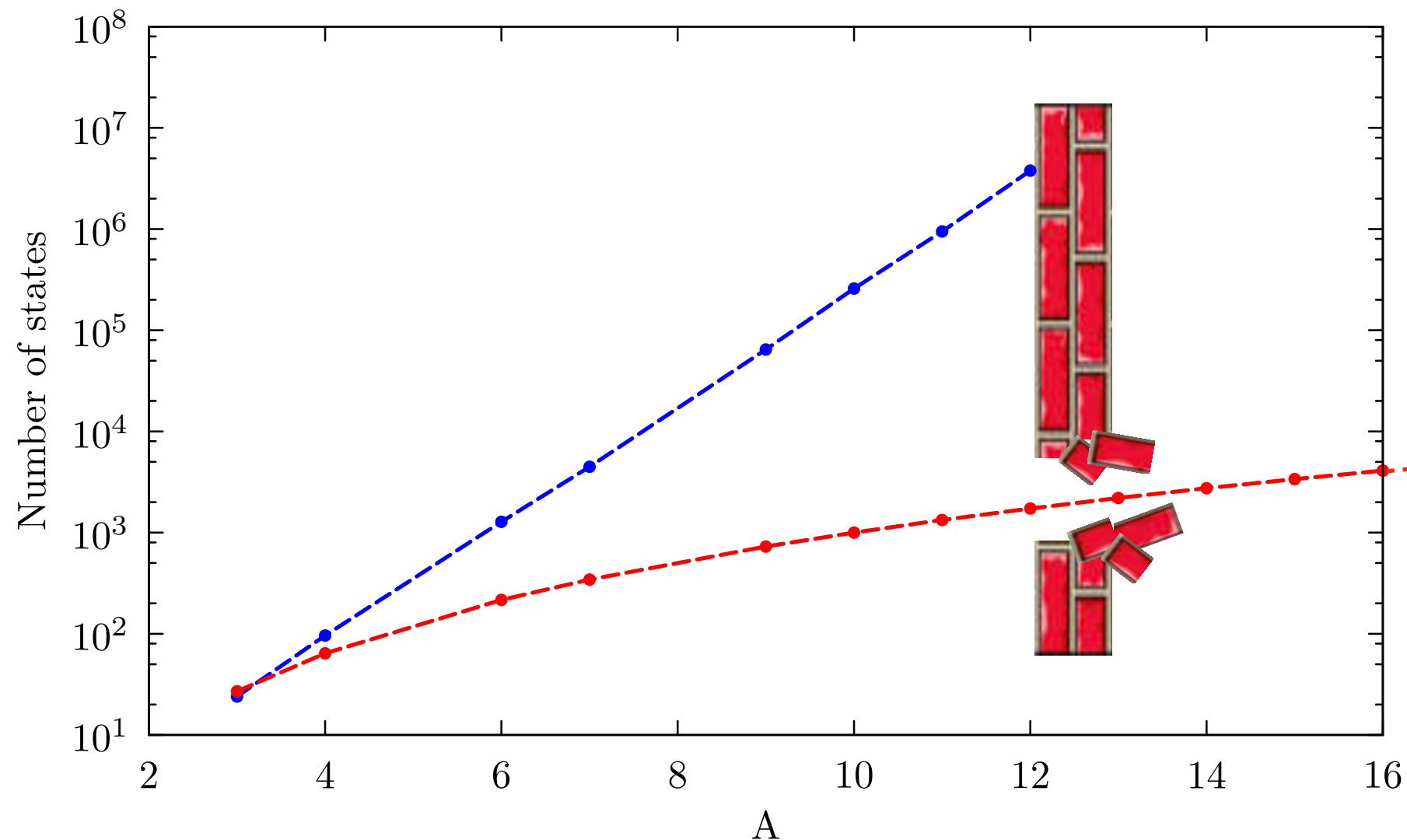
- **Green's function Monte Carlo (GFMC)** explicitly sums over the spin-isospin degrees of freedom

* Very accurate but limited to ^{12}C



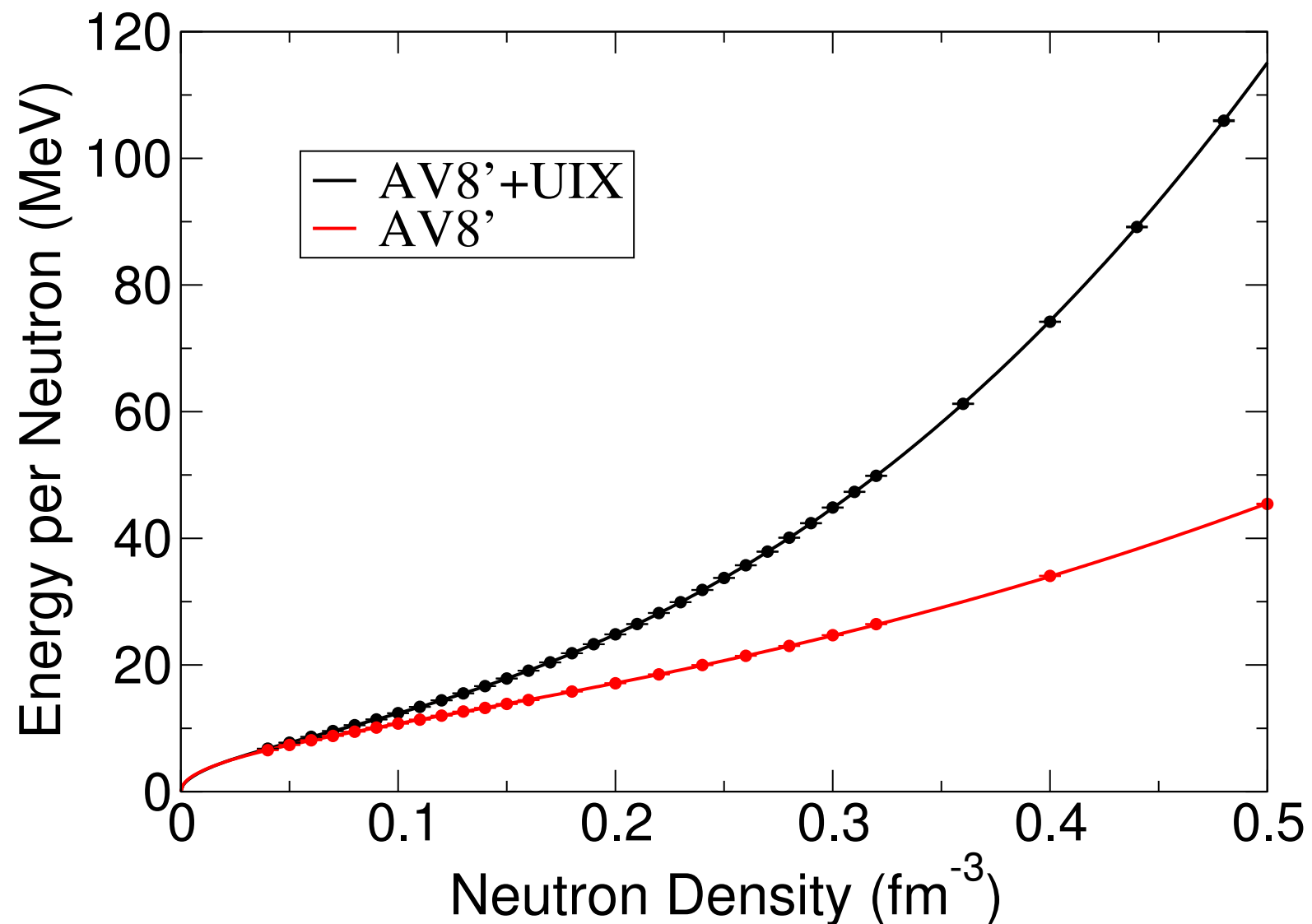
Quantum Monte Carlo

- **Green's function Monte Carlo (GFMC)** explicitly sums over the spin-isospin degrees of freedom
 - * Very accurate but limited to ^{12}C
- **Auxiliary field diffusion Monte Carlo (AFDMC)** samples the spin-isospin degrees of freedom
 - * Medium-mass nuclei, infinite (isospin-symmetric and asymmetric) nuclear matter



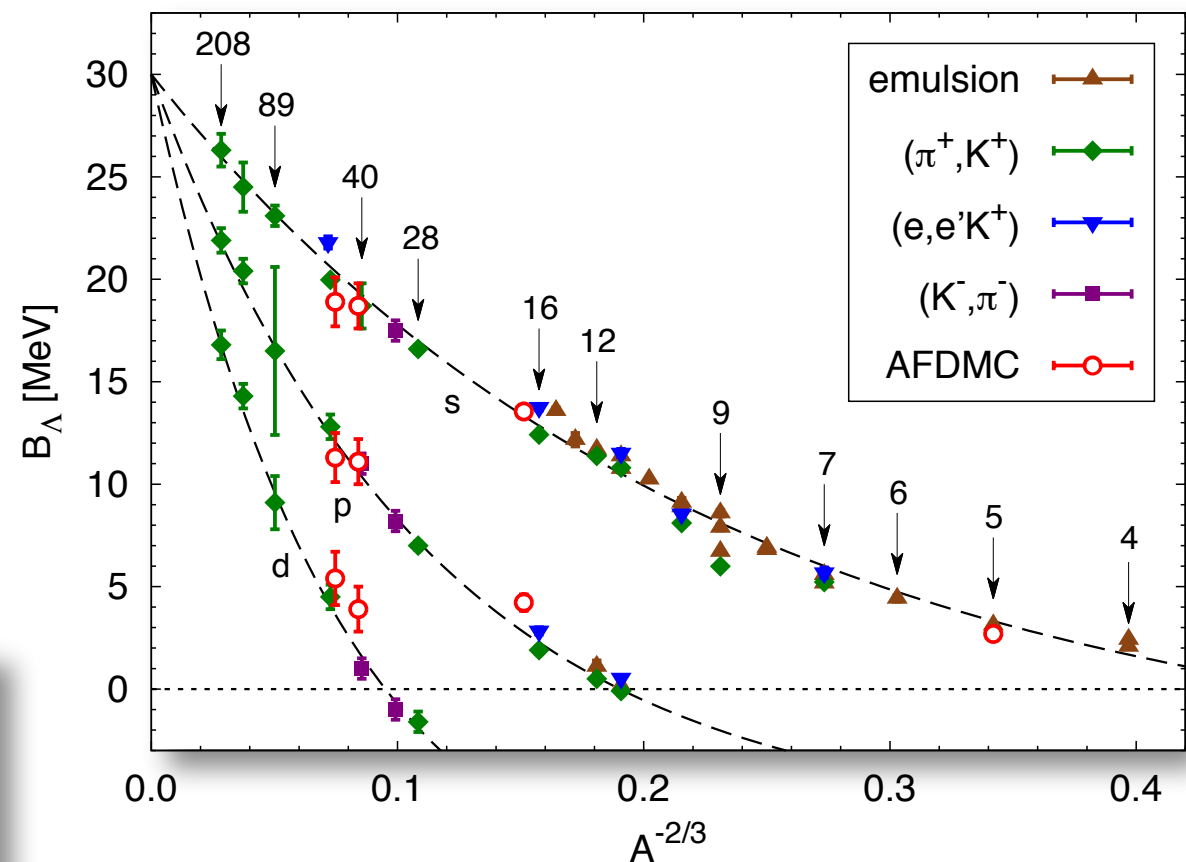
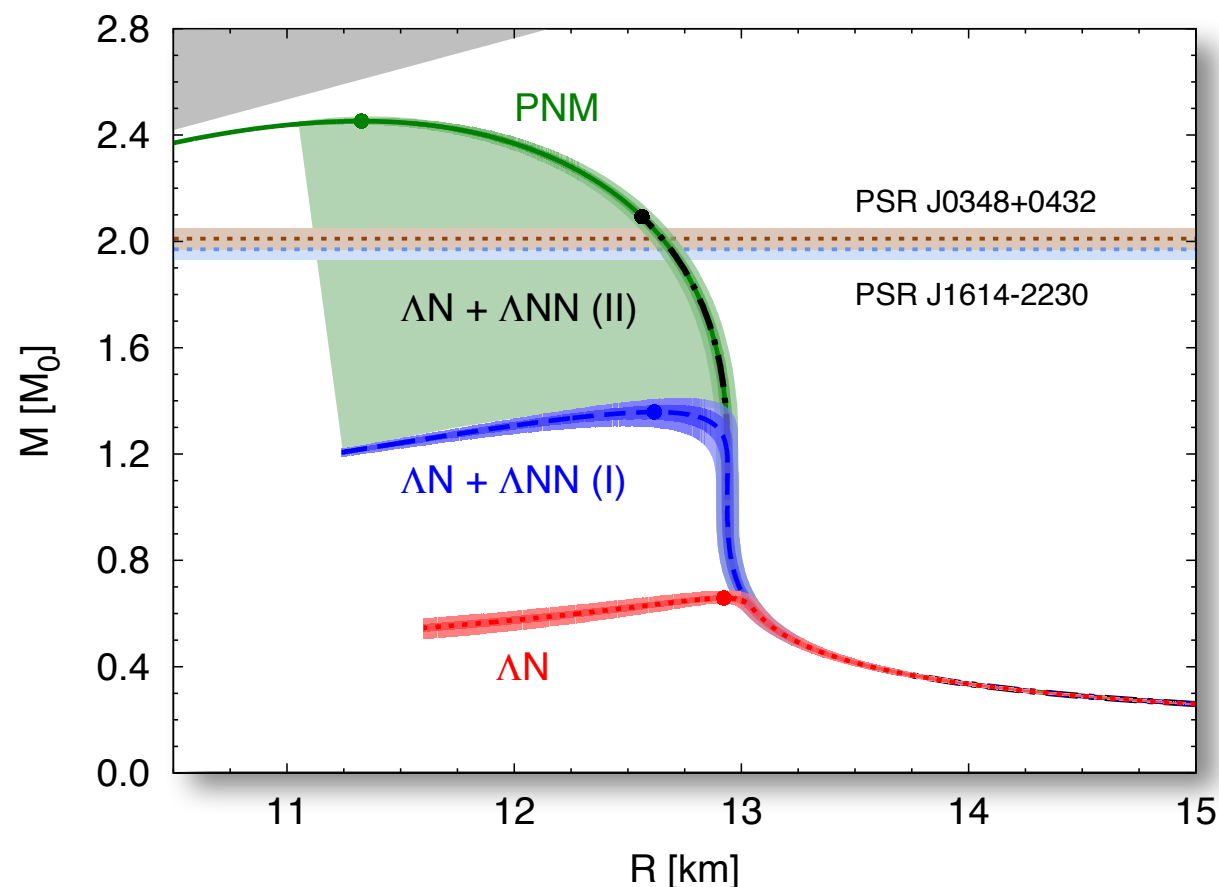
Quantum Monte Carlo

- Quantum Monte Carlo has been successfully applied to study infinite matter



Diffusion Monte Carlo: hyperons

- By fitting the hyperon-nucleon-nucleon force on the s-wave lambda-separation energy of $^{17}_{\Lambda}\text{O}$ and $^3_{\Lambda}\text{He}$ we can reproduce the experimental results over a wide-mass range.



- The hyperon-nucleon-nucleon force plays a fundamental role in the softening of the Equation of State and the consequent reduction of the neutron star maximum mass.
- More data are needed to assess the onset of hyperons in neutron stars

Chapter 5

How do we compute the electroweak
response functions?

Integral transform techniques

- We want to compute the following response functions (non-relativistic limit of the hadronic tensor)

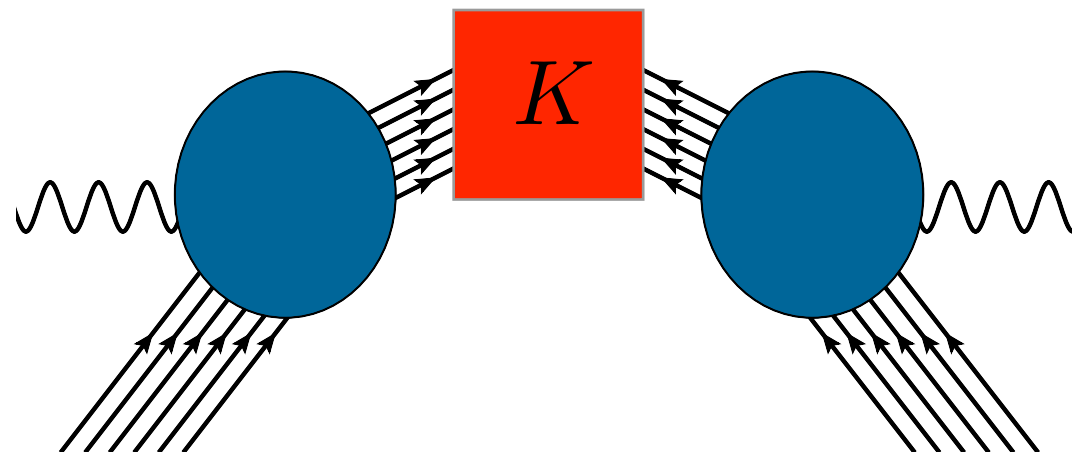
$$R_{\alpha\beta}(\omega, \mathbf{q}) = \sum_f \langle \Psi_0 | J_{\alpha}^{\dagger}(\mathbf{q}) | \Psi_f \rangle \langle \Psi_f | J_{\beta}(\mathbf{q}) | \Psi_0 \rangle \delta(\omega - E_f + E_0)$$

- The integral transform of the response function are generally defined as

$$E_{\alpha\beta}(\sigma, \mathbf{q}) \equiv \int d\omega K(\sigma, \omega) R_{\alpha\beta}(\omega, \mathbf{q})$$

- Using the completeness of the final states, they can be expressed in terms of ground-state expectation values

$$E_{\alpha\beta}(\sigma, \mathbf{q}) = \langle \Psi_0 | J_{\alpha}^{\dagger}(\mathbf{q}) K(\sigma, H - E_0) J_{\beta}(\mathbf{q}) | \Psi_0 \rangle$$



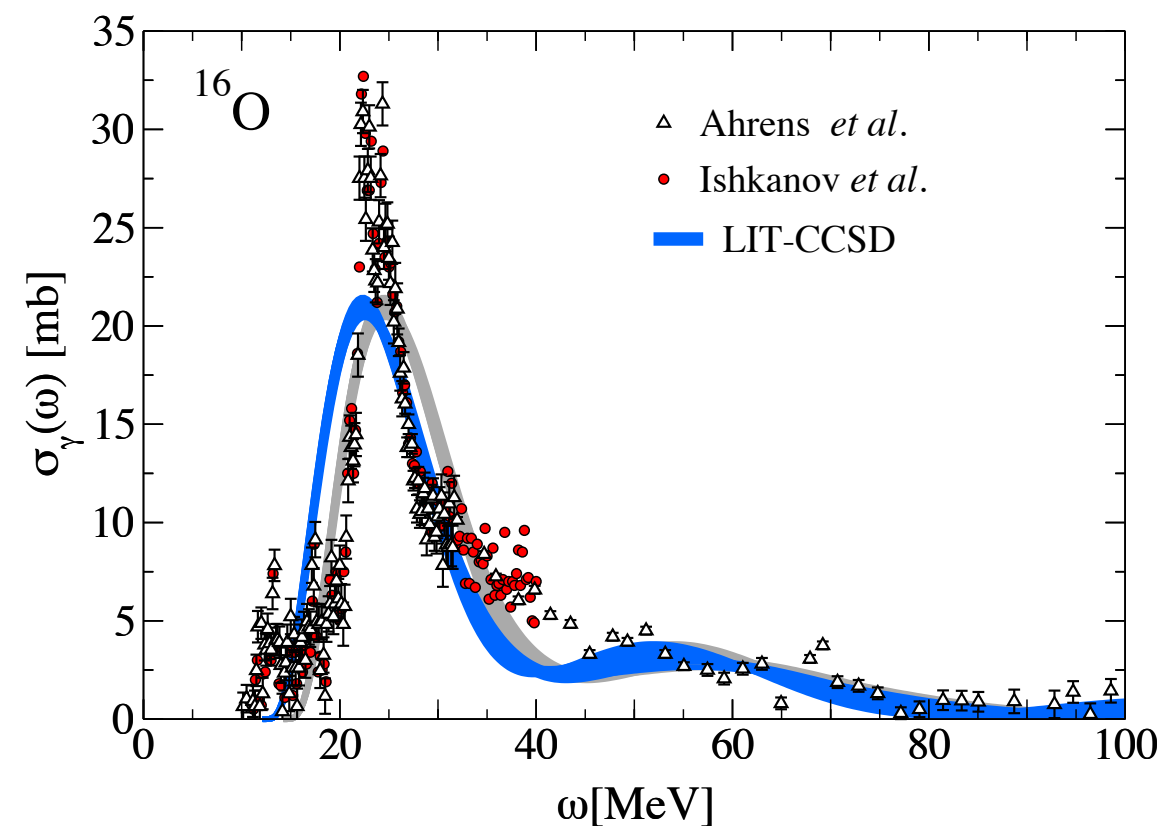
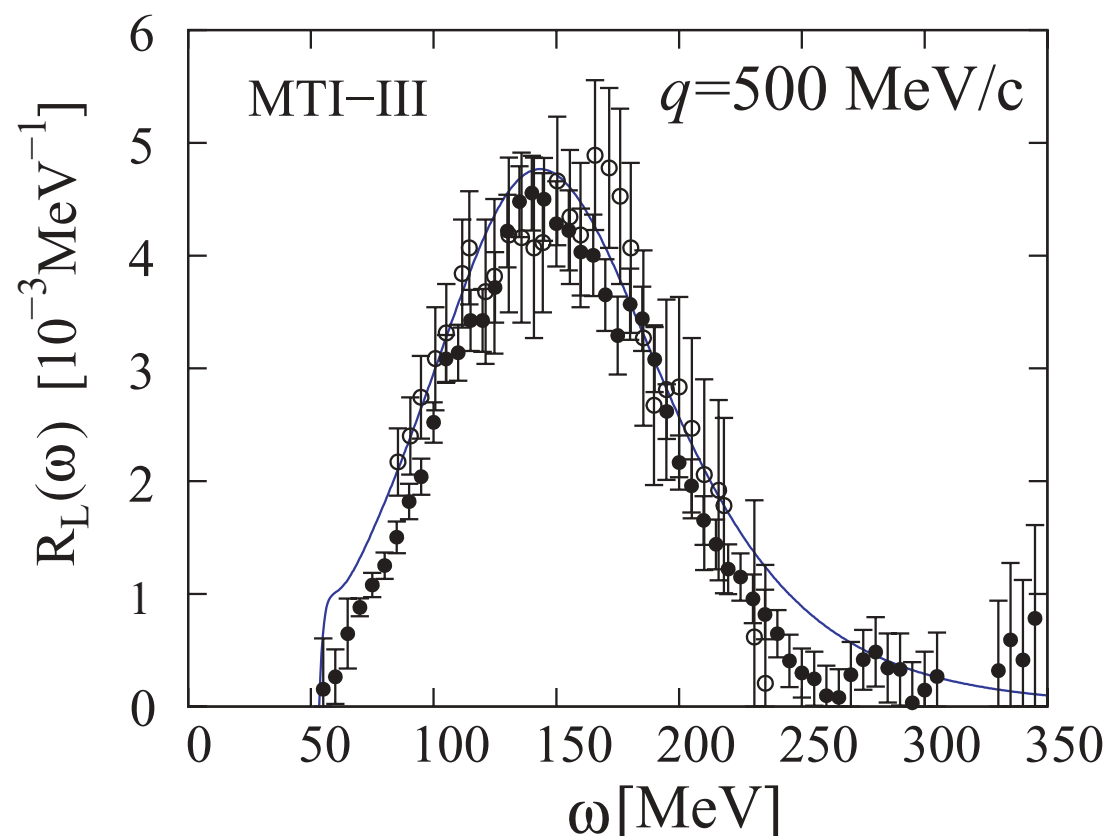
Lorentz integral transform (LIT)

- The Lorentz integral transform

$$K(\sigma, \omega) = \frac{1}{(\omega - \sigma_R)^2 + \sigma_I^2}$$

has been successfully exploited in the calculation of electromagnetic and neutral-weak responses of light nuclei.

- More recently, in combination with the coupled-cluster method, Lorentz integral transform has been applied to compute the giant dipole resonances of nuclei as large as ^{16}O , ^{22}O and ^{40}Ca .

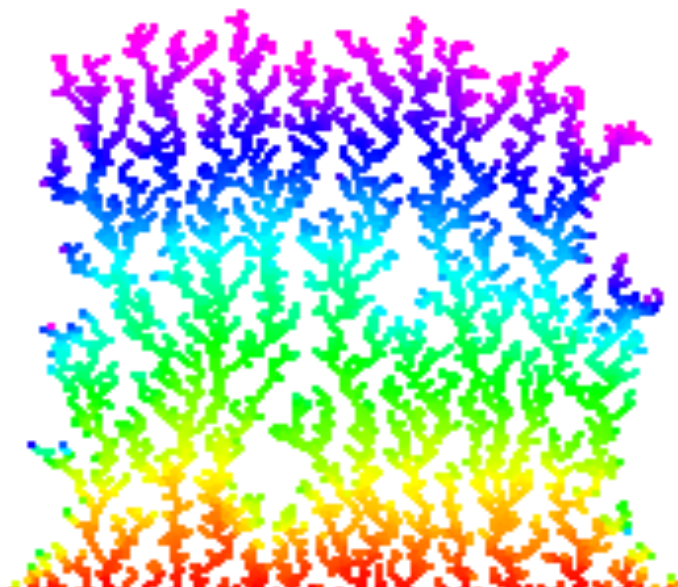
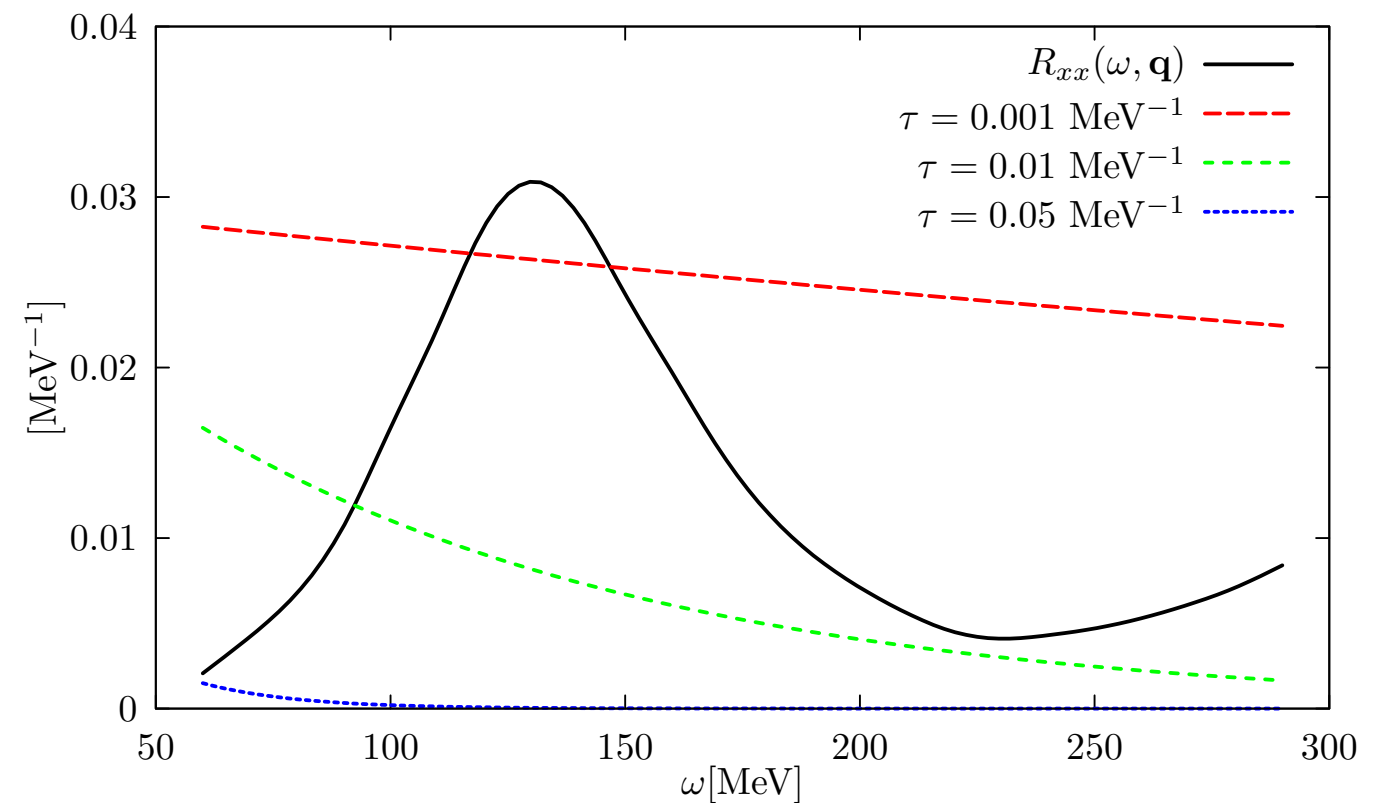


Euclidean response function

Valuable information on the energy dependence of the response functions can be inferred from their Laplace transforms

$$E_{\alpha\beta}(\tau, \mathbf{q}) \equiv \int d\omega e^{-\omega\tau} R_{\alpha\beta}(\omega, \mathbf{q})$$

At finite imaginary time the contributions from large energy transfer are quickly suppressed



The system is first heated up by the transition operator. Its cooling determines the Euclidean response of the system

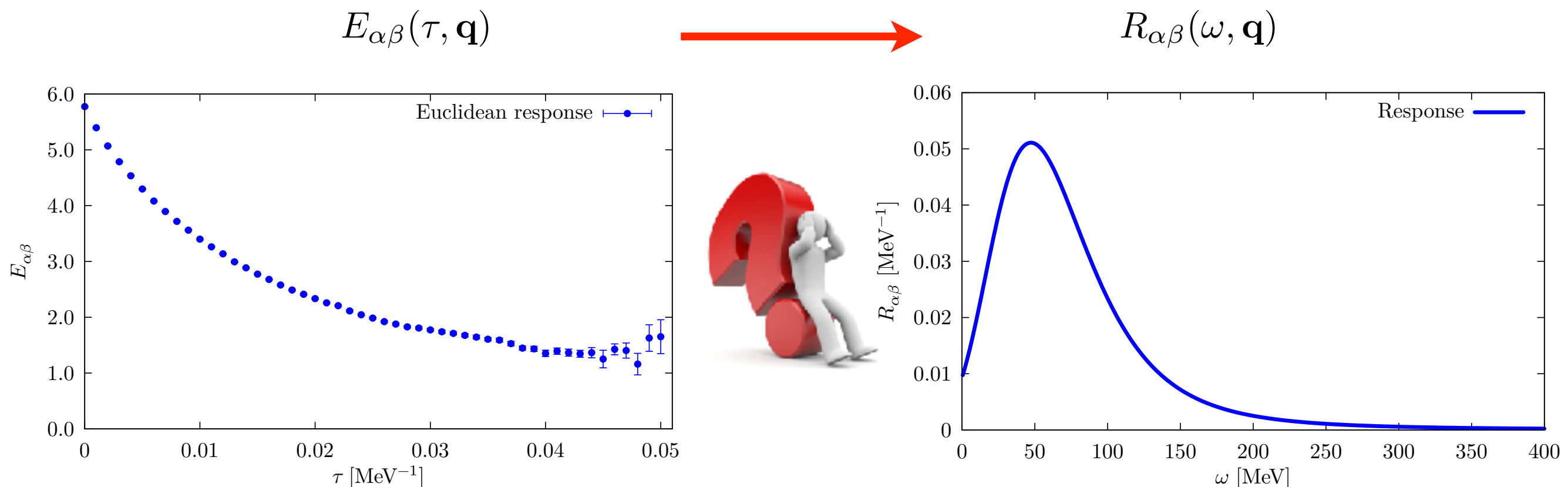
$$E_{\alpha\beta}(\tau, \mathbf{q}) = \langle \Psi_0 | J_{\alpha}^{\dagger}(\mathbf{q}) e^{-(H-E_0)\tau} J_{\beta}(\mathbf{q}) | \Psi_0 \rangle$$

Same technique used in Lattice QCD, condensed matter physics...

Inversion of the Euclidean response

The Euclidean response formalism allows one to extract dynamical properties of the system from ground-state calculations

Inverting the Euclidean response is an ill posed problem: any set of observations is limited and noisy and the situation is even worse since the kernel is a smoothing operator.



We have found **maximum entropy technique** to be best suited for our purposes.

Image reconstruction from incomplete and noisy data

S. F. Gull & G. J. Daniell*

Mullard Radio Astronomy Observatory, Cavendish Laboratory, Madingley Road, Cambridge, UK

Results are presented of a powerful technique for image reconstruction by a maximum entropy method, which is sufficiently fast to be useful for large and complicated images. Although our examples are taken from the fields of radio and X-ray astronomy, the technique is immediately applicable in spectroscopy, electron microscopy, X-ray crystallography, geophysics and virtually any type of optical image processing. Applied to radioastronomical data, the algorithm reveals details not seen by conventional analysis, but which are known to exist.

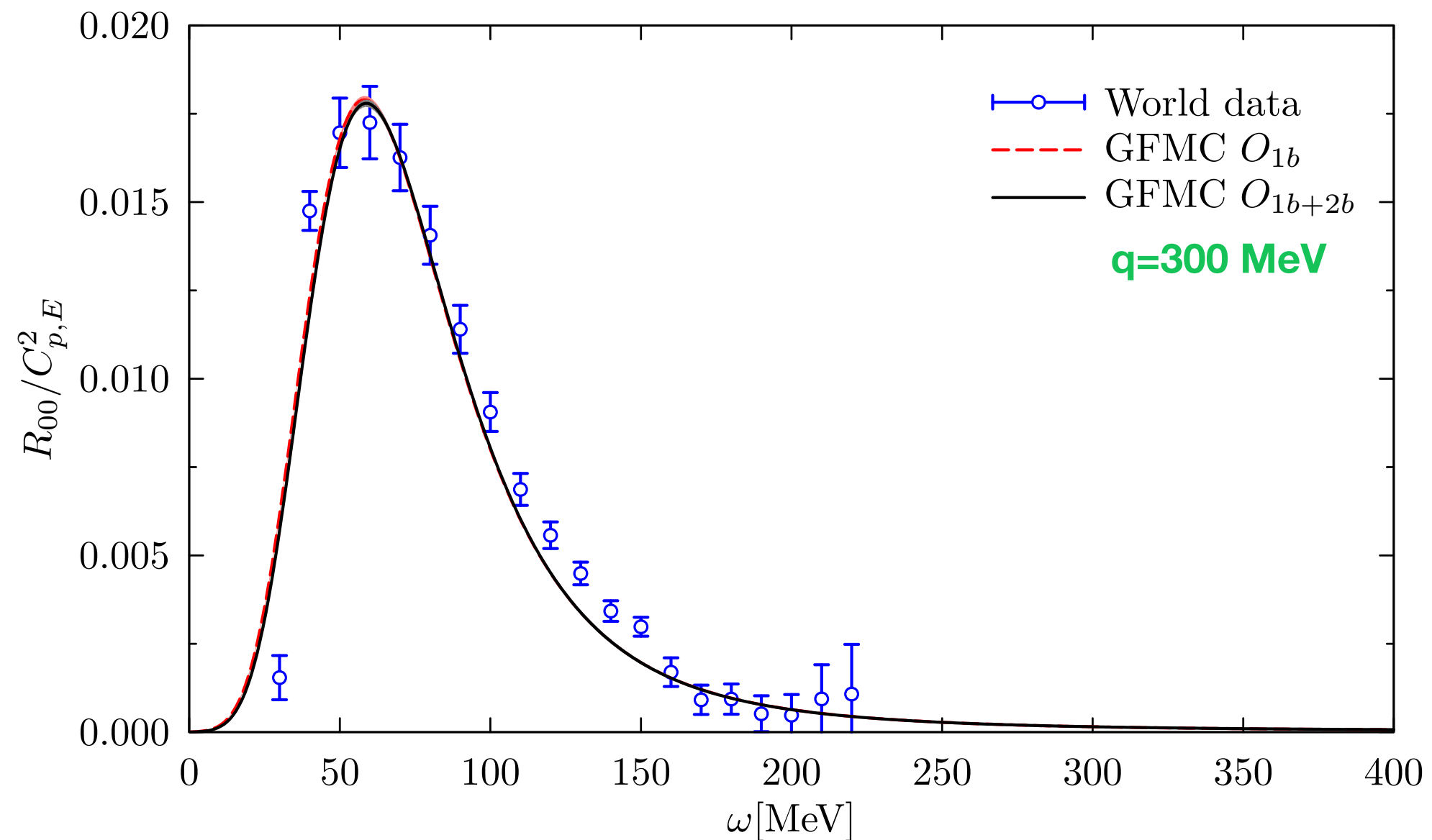
To avoid abstraction, we shall refer to our radioastronomical example. Starting with incomplete and noisy data, one can obtain by the Backus–Gilbert method a series of maps of the distribution of radio brightness across the sky, all of which are consistent with the data, but have different resolutions and noise levels. From the data alone, there is no reason to prefer any one of these maps, and the observer may select the most appropriate one to answer any specific question. Hence, the method cannot produce a unique ‘best’ map of the sky. There is no single map that is equally suitable for discussing both accurate flux measurements and source positions.

Nevertheless, it is useful to have a single general-purpose map of the sky, and the maximum-entropy map described here fulfils

Nature, 272, 688 (1978)

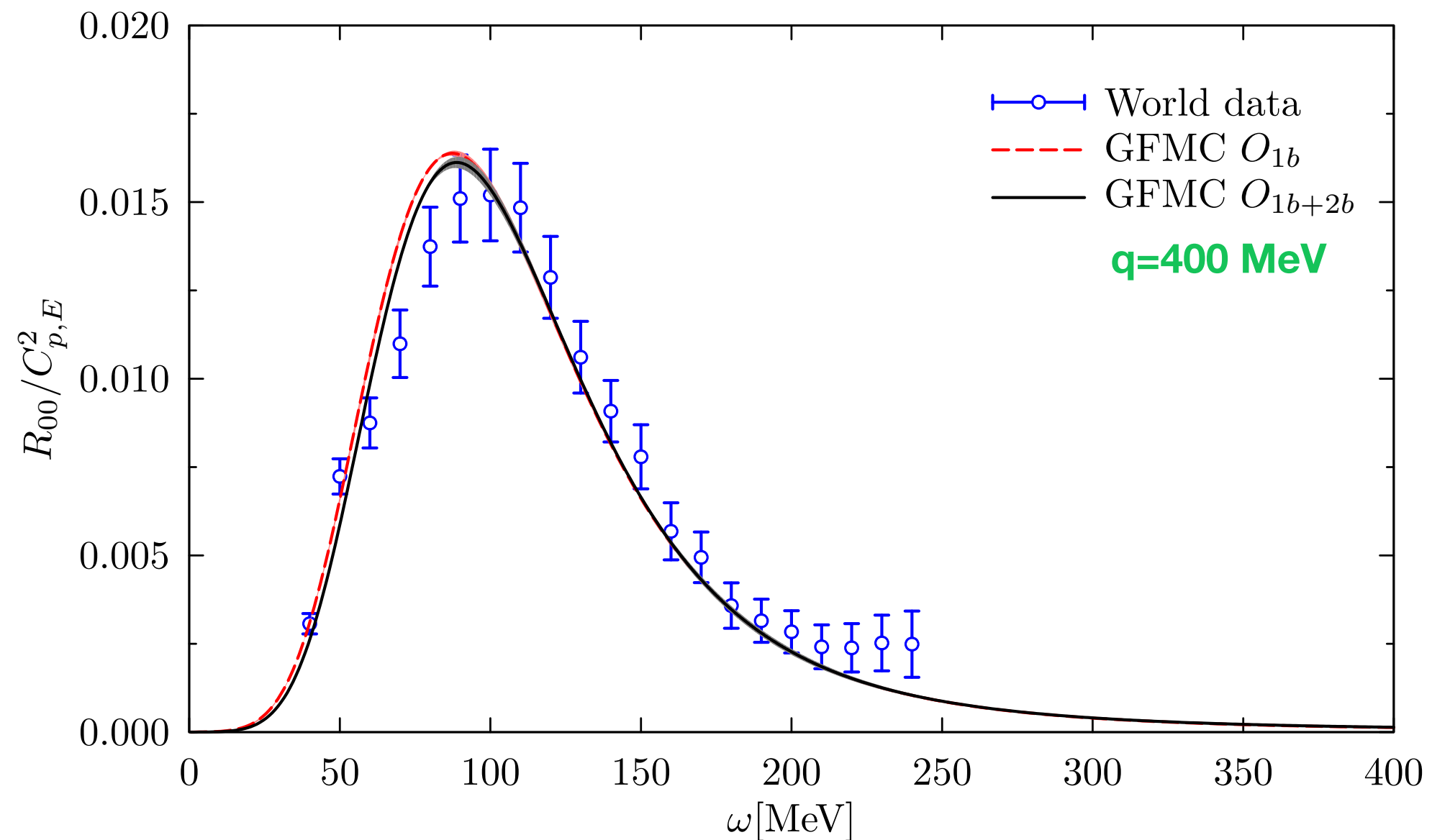
^4He electromagnetic response

Two-body currents do not provide significant changes in the longitudinal response.
The agreement with experimental data appears to be remarkably good.



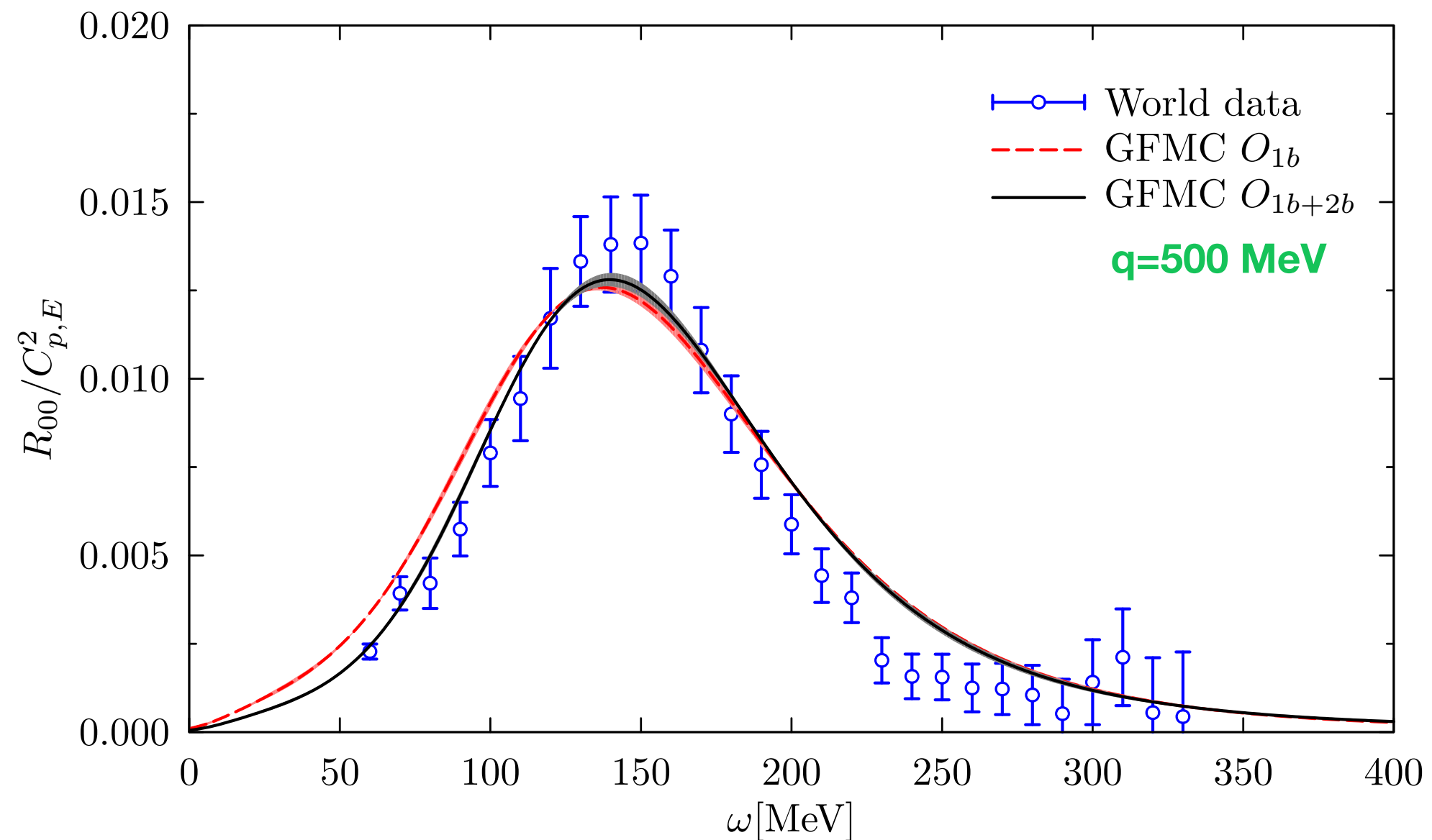
^4He electromagnetic response

Two-body currents do not provide significant changes in the longitudinal response.
The agreement with experimental data appears to be remarkably good.



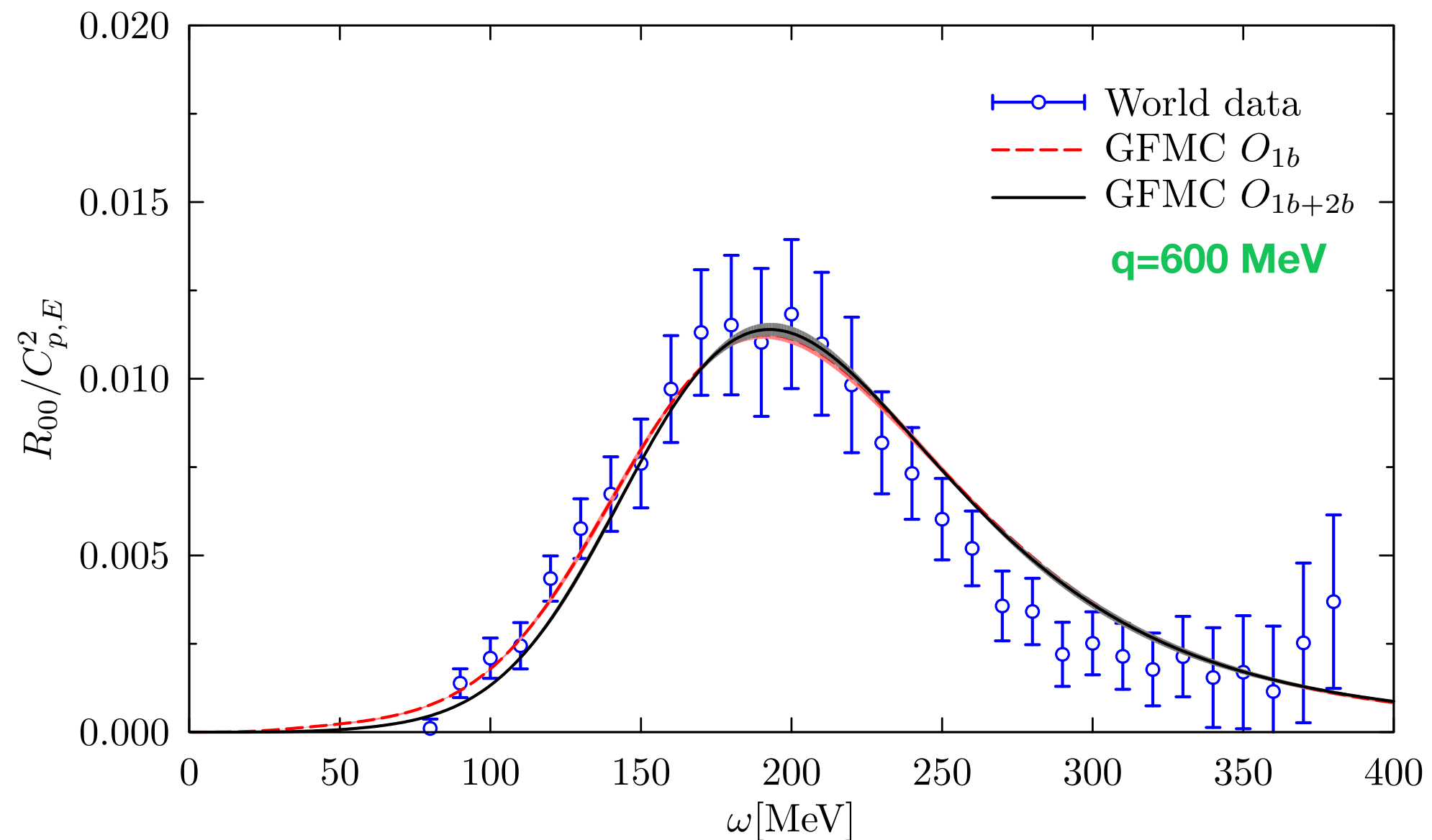
^4He electromagnetic response

Two-body currents do not provide significant changes in the longitudinal response.
The agreement with experimental data appears to be remarkably good.



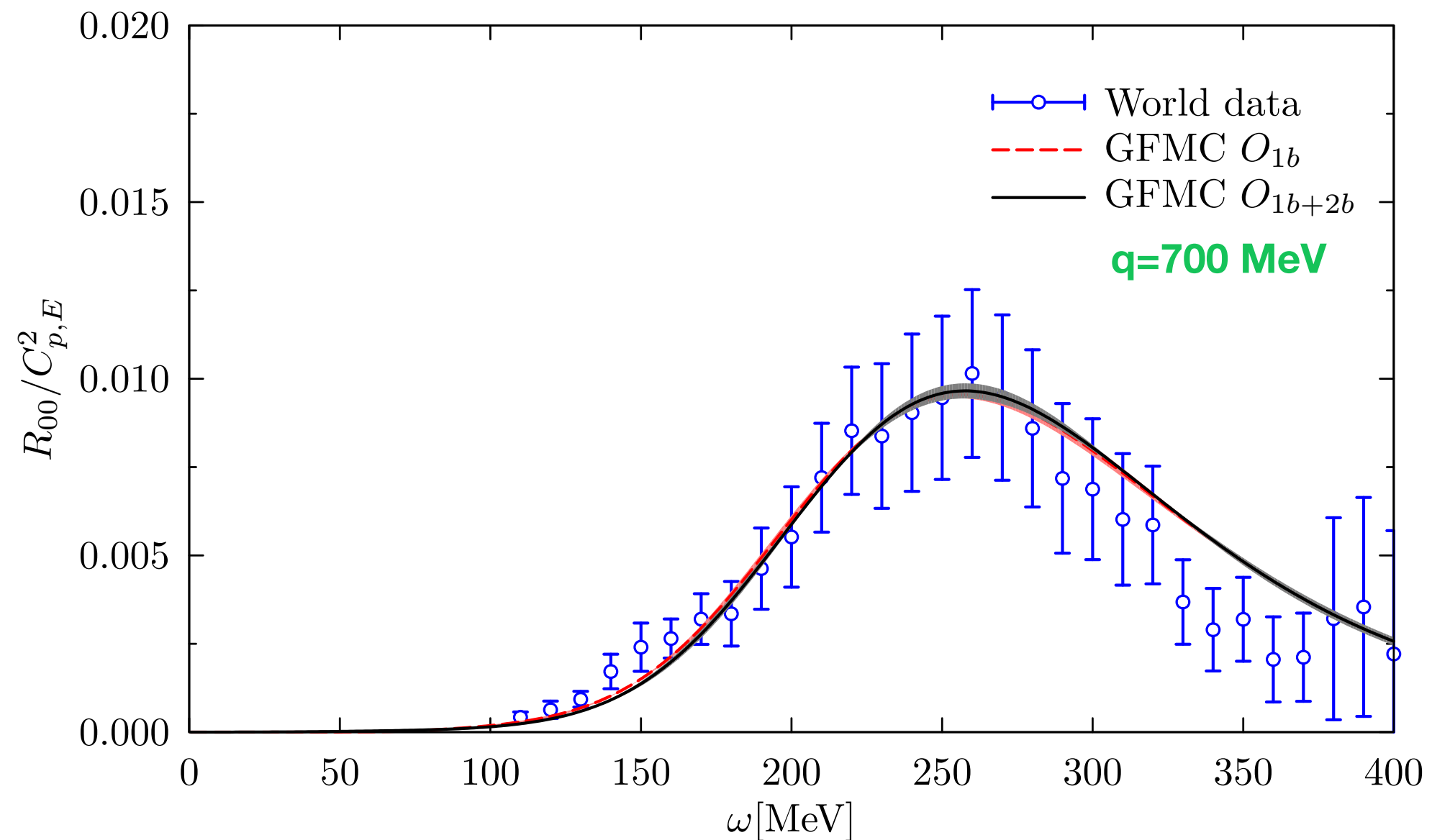
^4He electromagnetic response

Two-body currents do not provide significant changes in the longitudinal response.
The agreement with experimental data appears to be remarkably good.



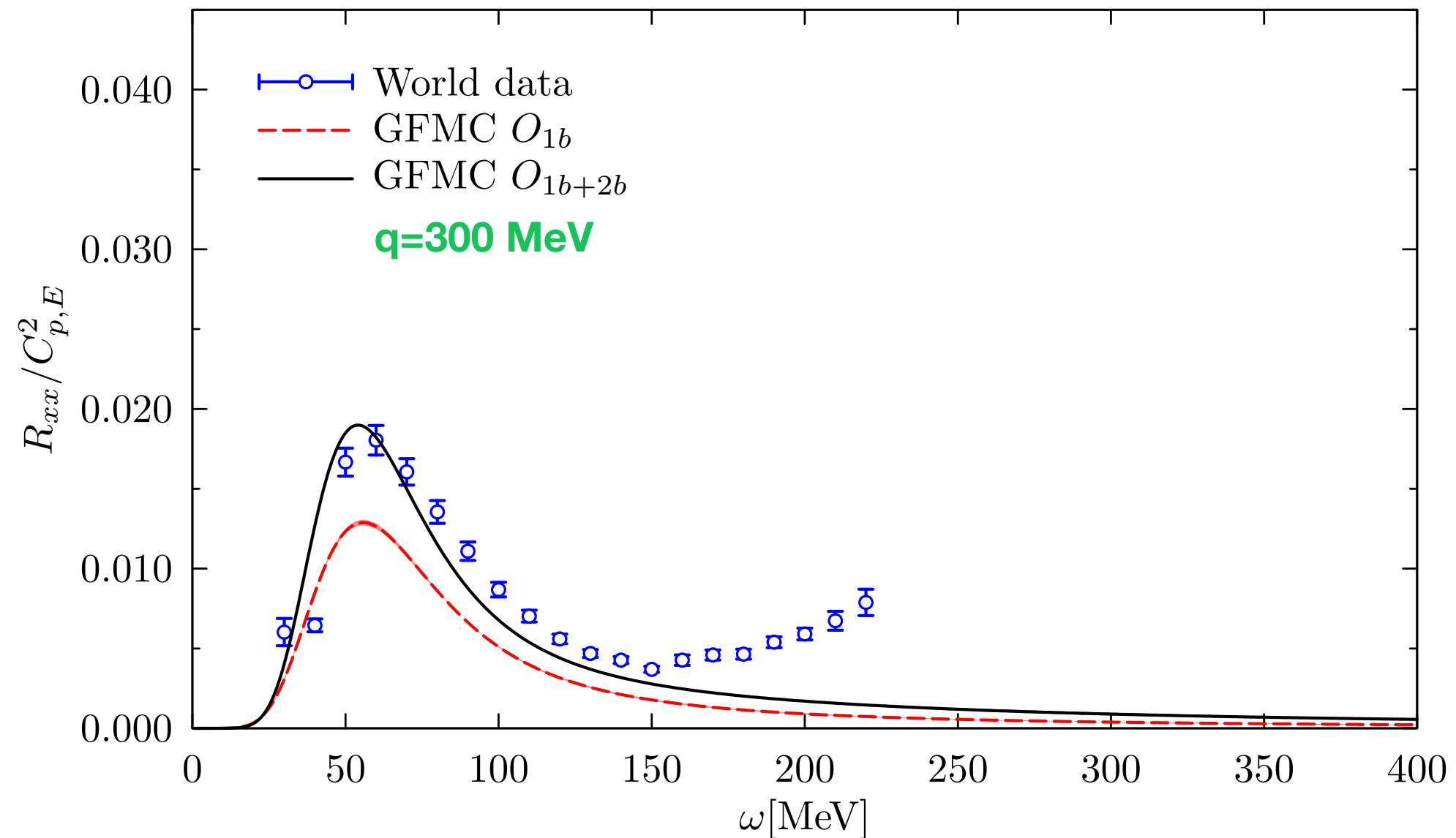
^4He electromagnetic response

Two-body currents do not provide significant changes in the longitudinal response.
The agreement with experimental data appears to be remarkably good.



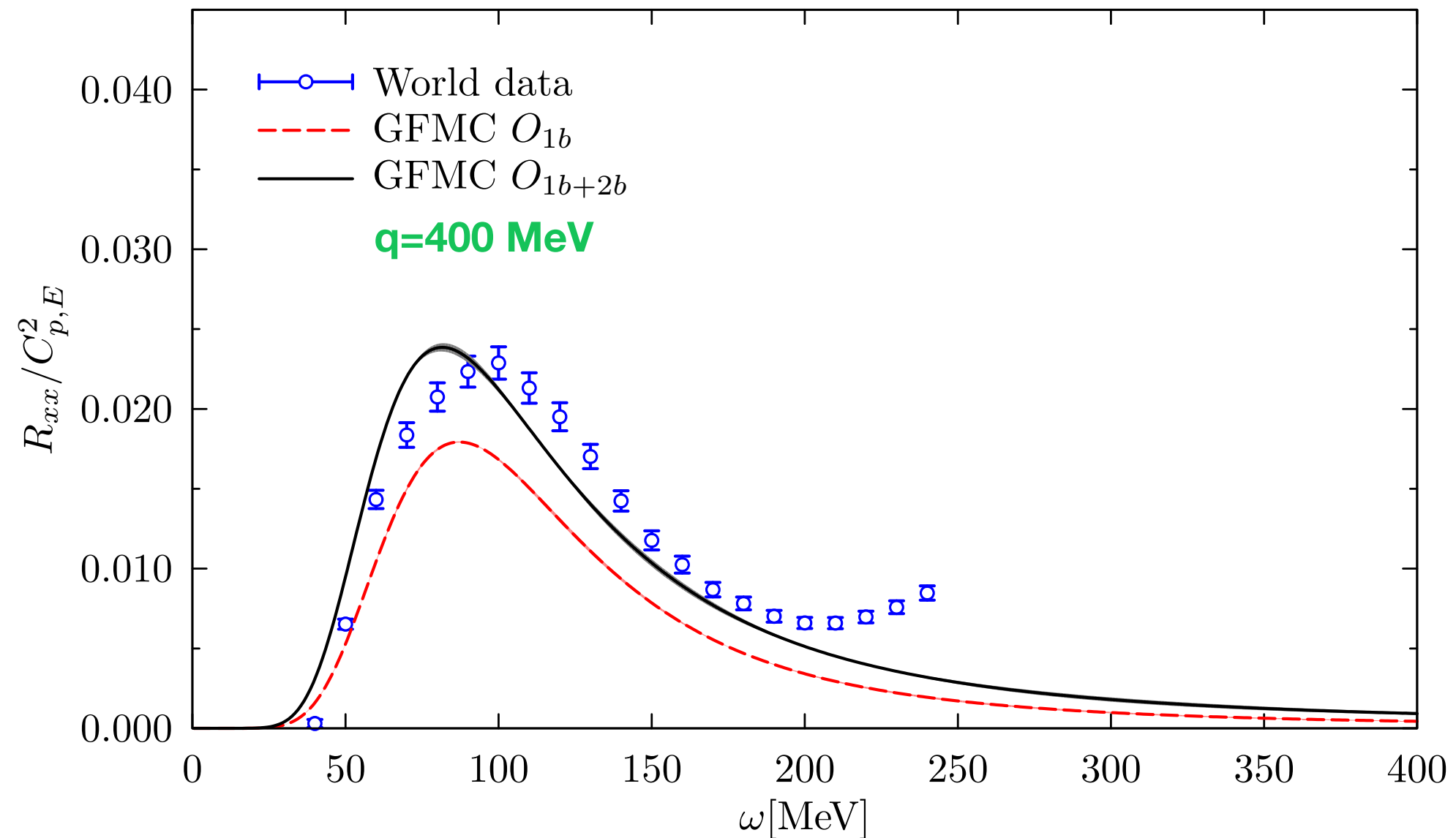
^4He electromagnetic response

Two-body currents significantly enhance the transverse response function, not only in the dip region, but also in the quasielastic peak and threshold regions.



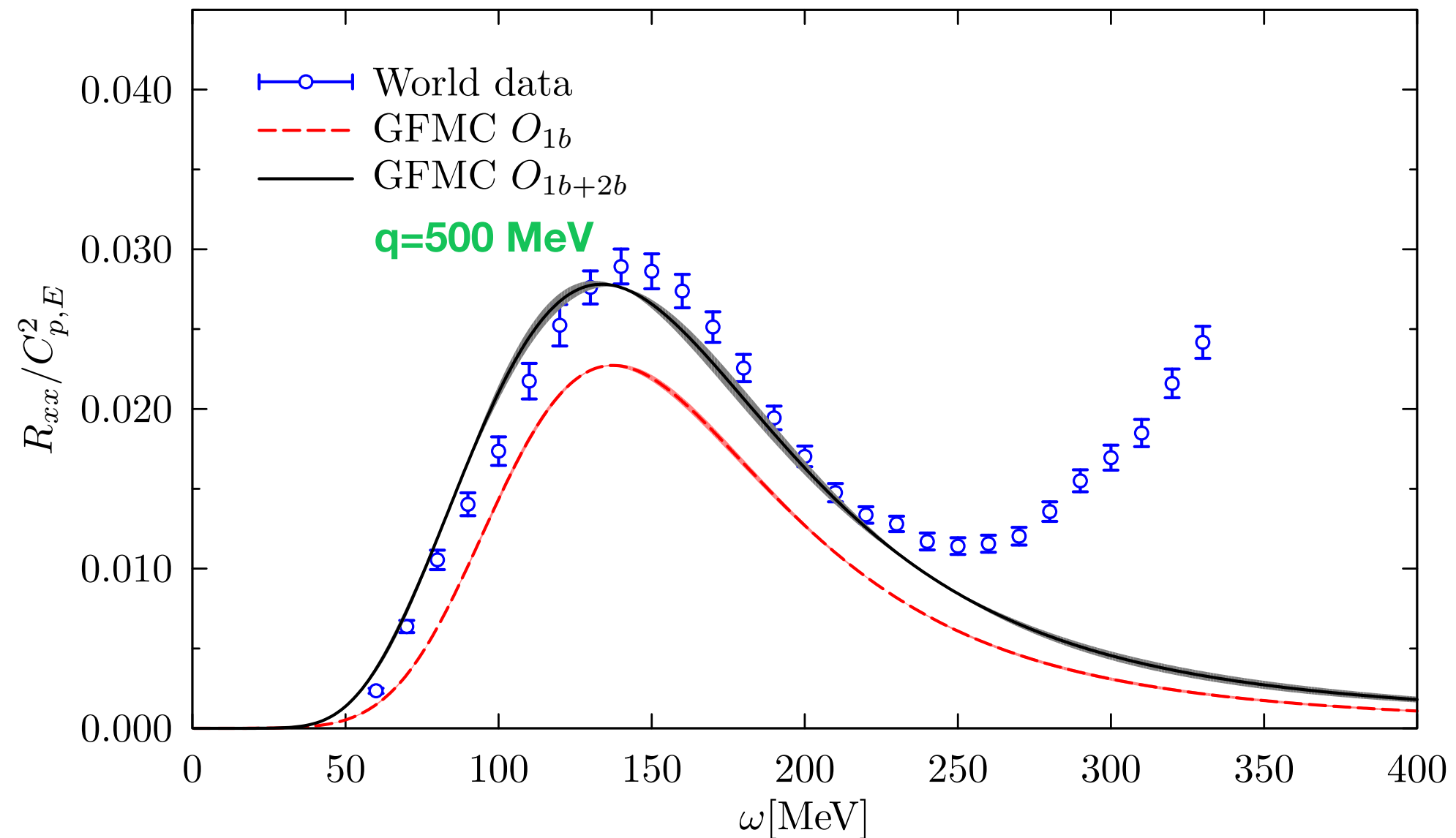
^4He electromagnetic response

Two-body currents significantly enhance the transverse response function, not only in the dip region, but also in the quasielastic peak and threshold regions.



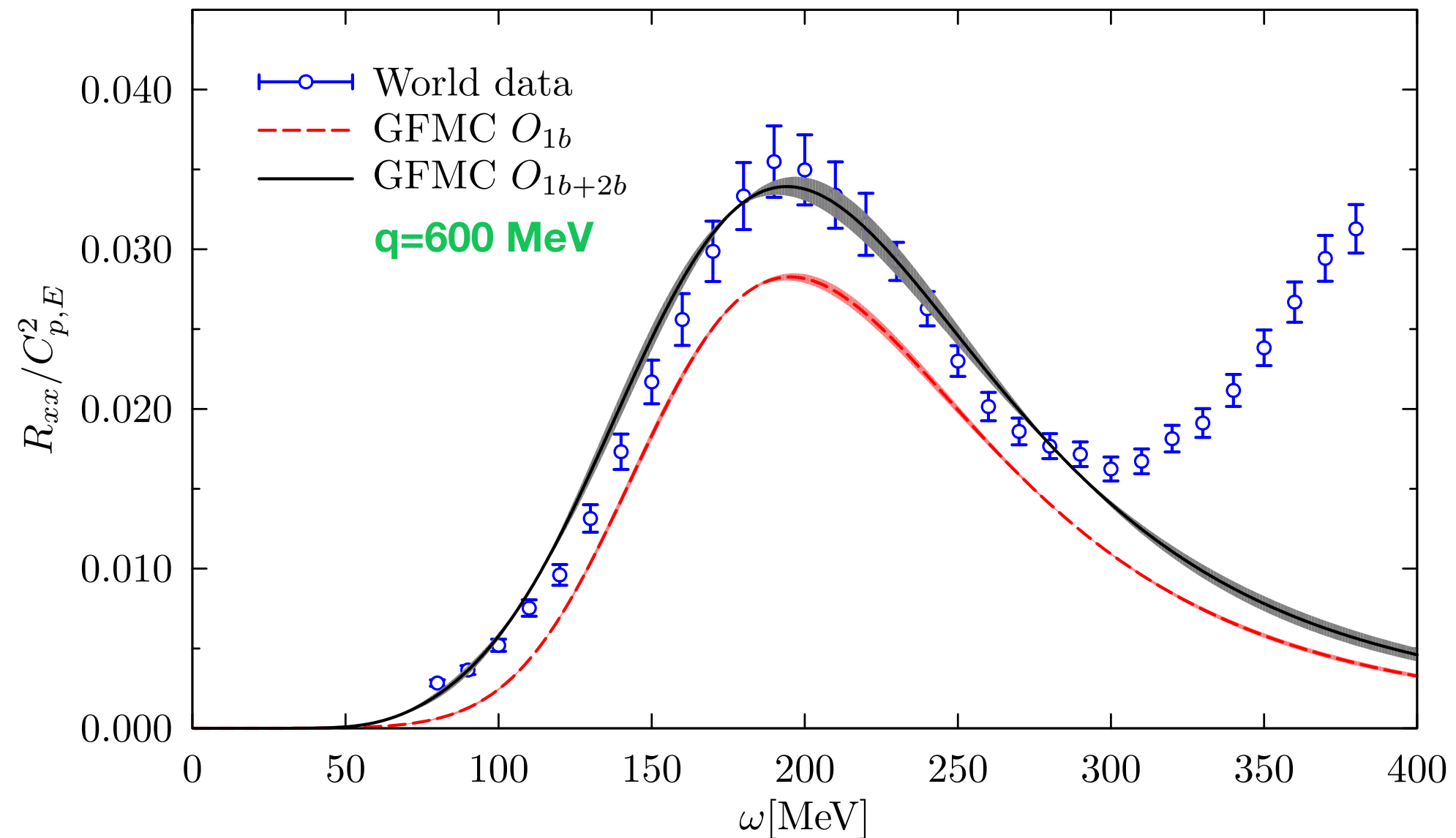
^4He electromagnetic response

Two-body currents significantly enhance the transverse response function, not only in the dip region, but also in the quasielastic peak and threshold regions.



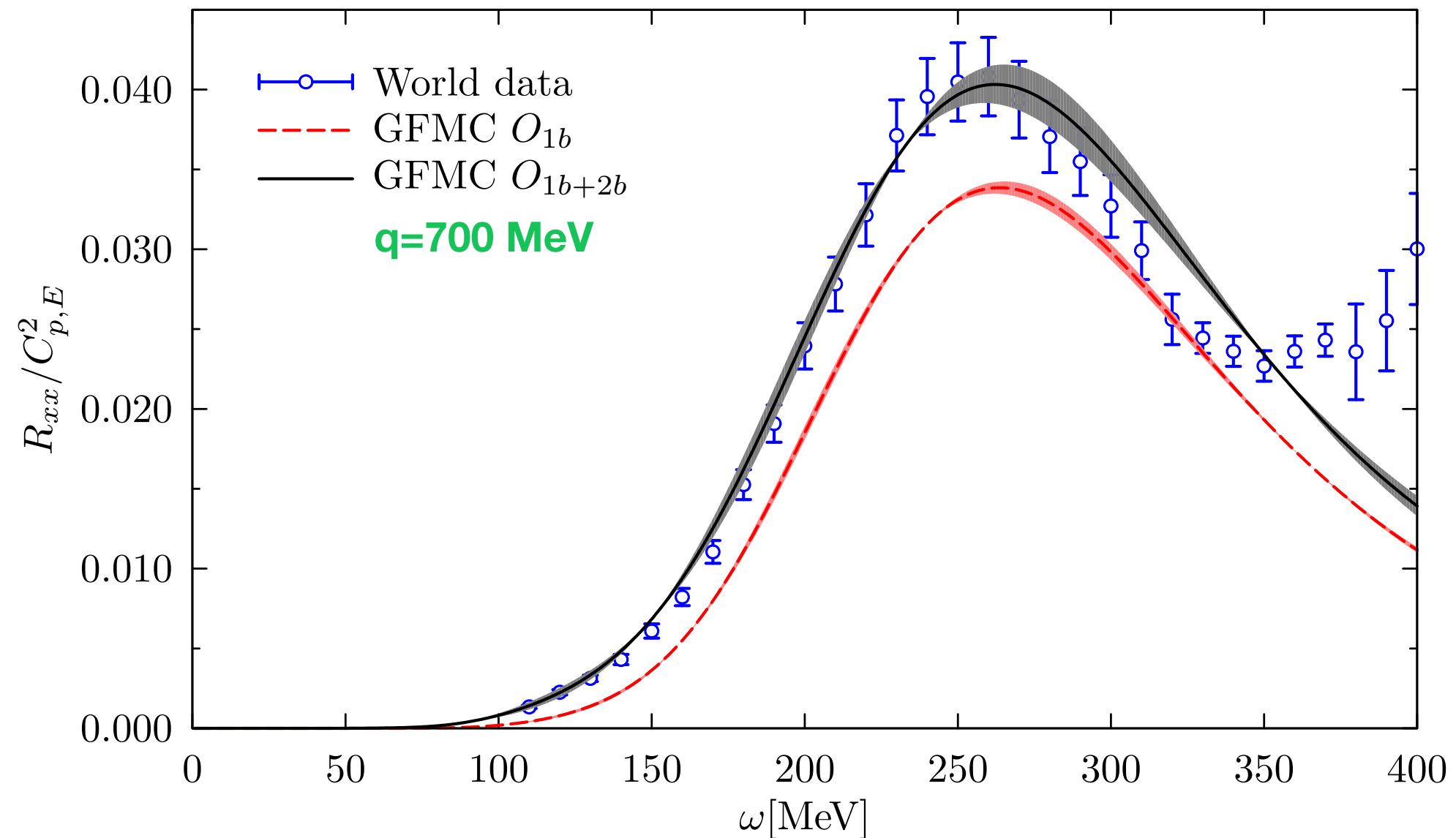
^4He electromagnetic response

Two-body currents significantly enhance the transverse response function, not only in the dip region, but also in the quasielastic peak and threshold regions.



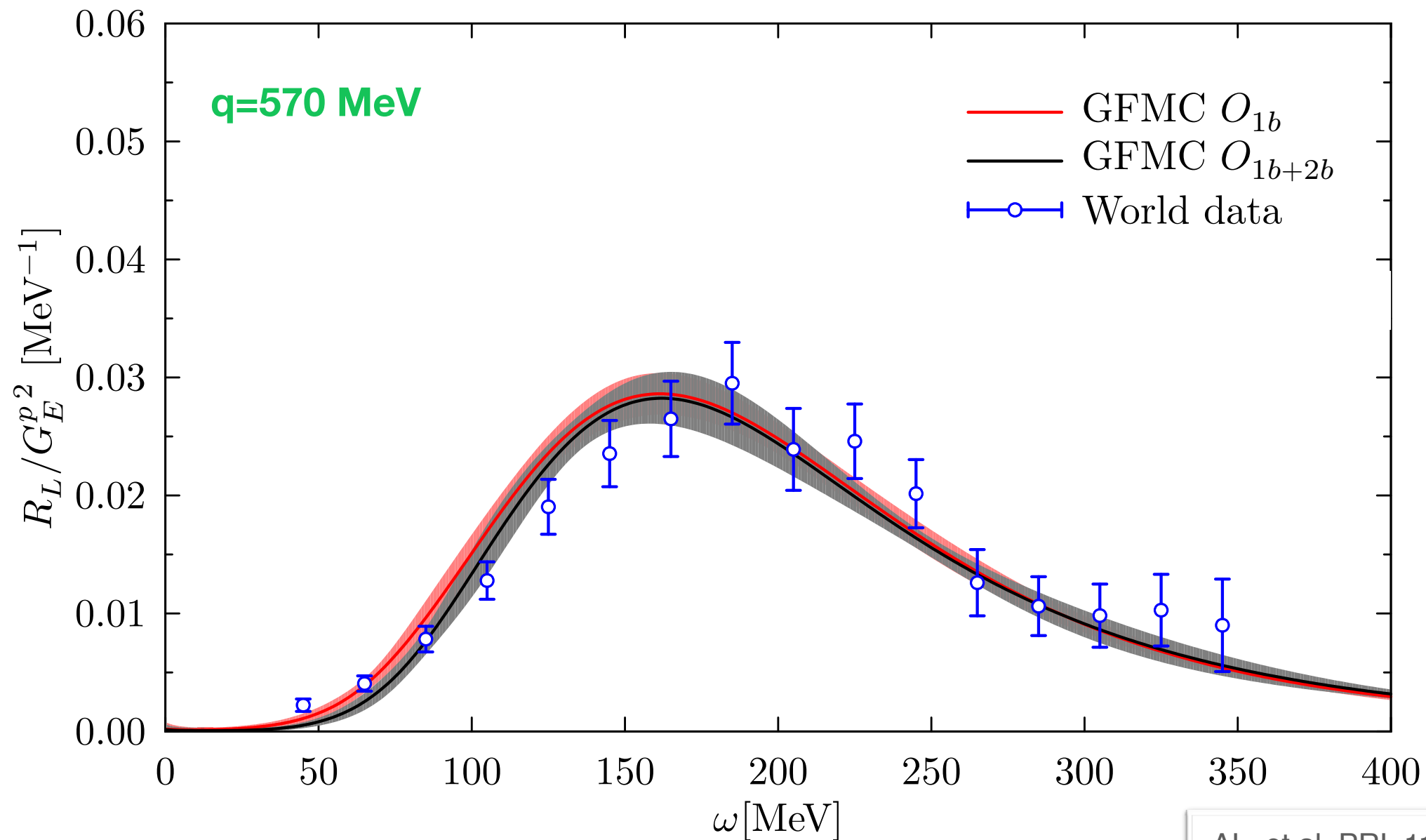
^4He electromagnetic response

Two-body currents significantly enhance the transverse response function, not only in the dip region, but also in the quasielastic peak and threshold regions.



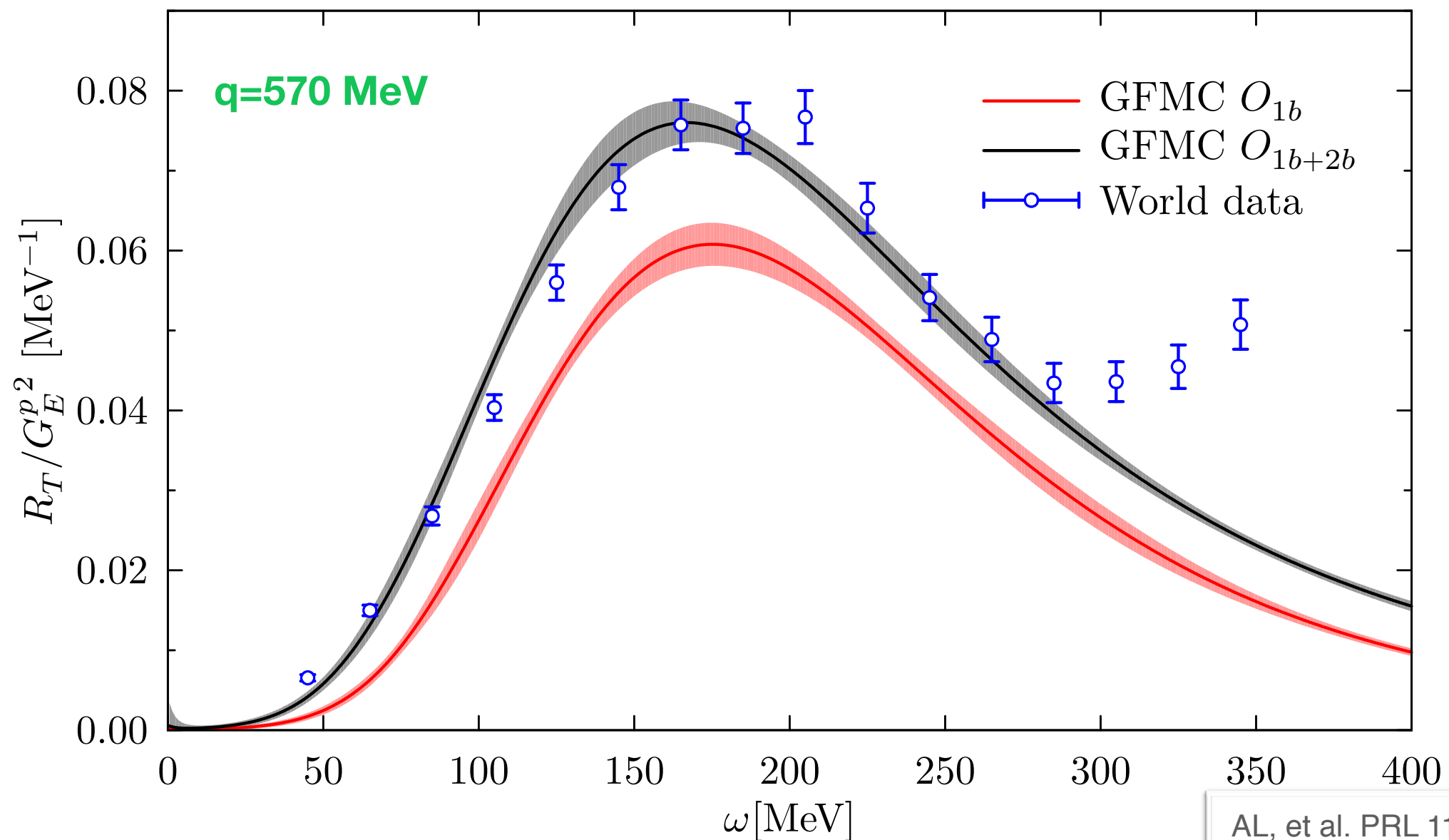
^{12}C electromagnetic response

- Very good agreement with the experimental data
- Small contribution from two-body currents to the transverse response functions.
- No quenching of the proton electric form factor!



^{12}C electromagnetic response

- Very good agreement with the experimental data.
- Sizable contribution from two-body currents to the transverse response functions.
- Hints for the axial mass puzzle

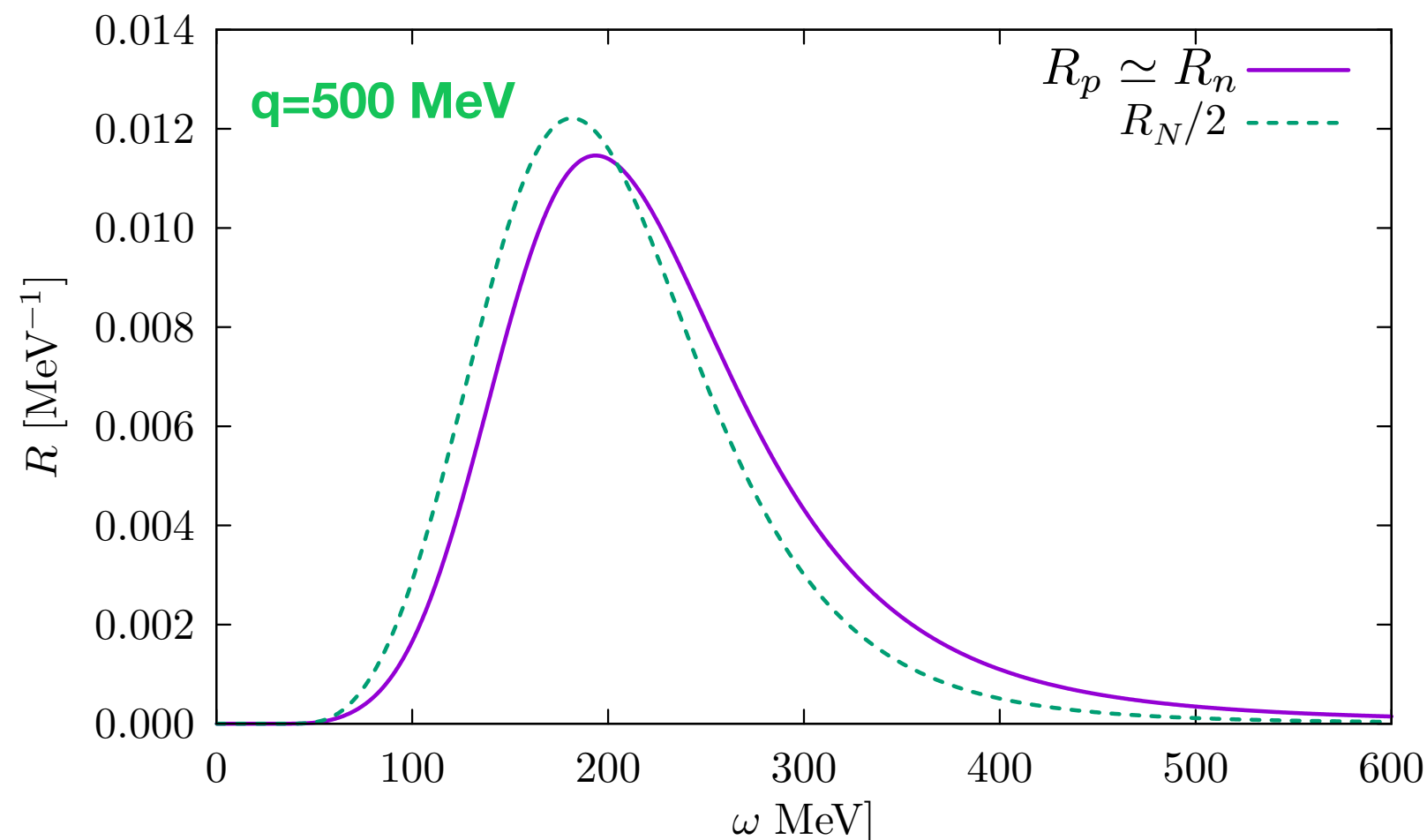


Nuclear dynamics surprises

- Beyond impulse approximation effects are important. Particularly enlightening is the comparison between the nucleon and proton responses

$$R_{N,p} \equiv \sum_f \langle 0 | \rho_{N,p}^\dagger(\mathbf{q}) | f \rangle \langle f | \rho_{N,p}(\mathbf{q}) | 0 \rangle \delta(E_0 + \omega - E_f)$$

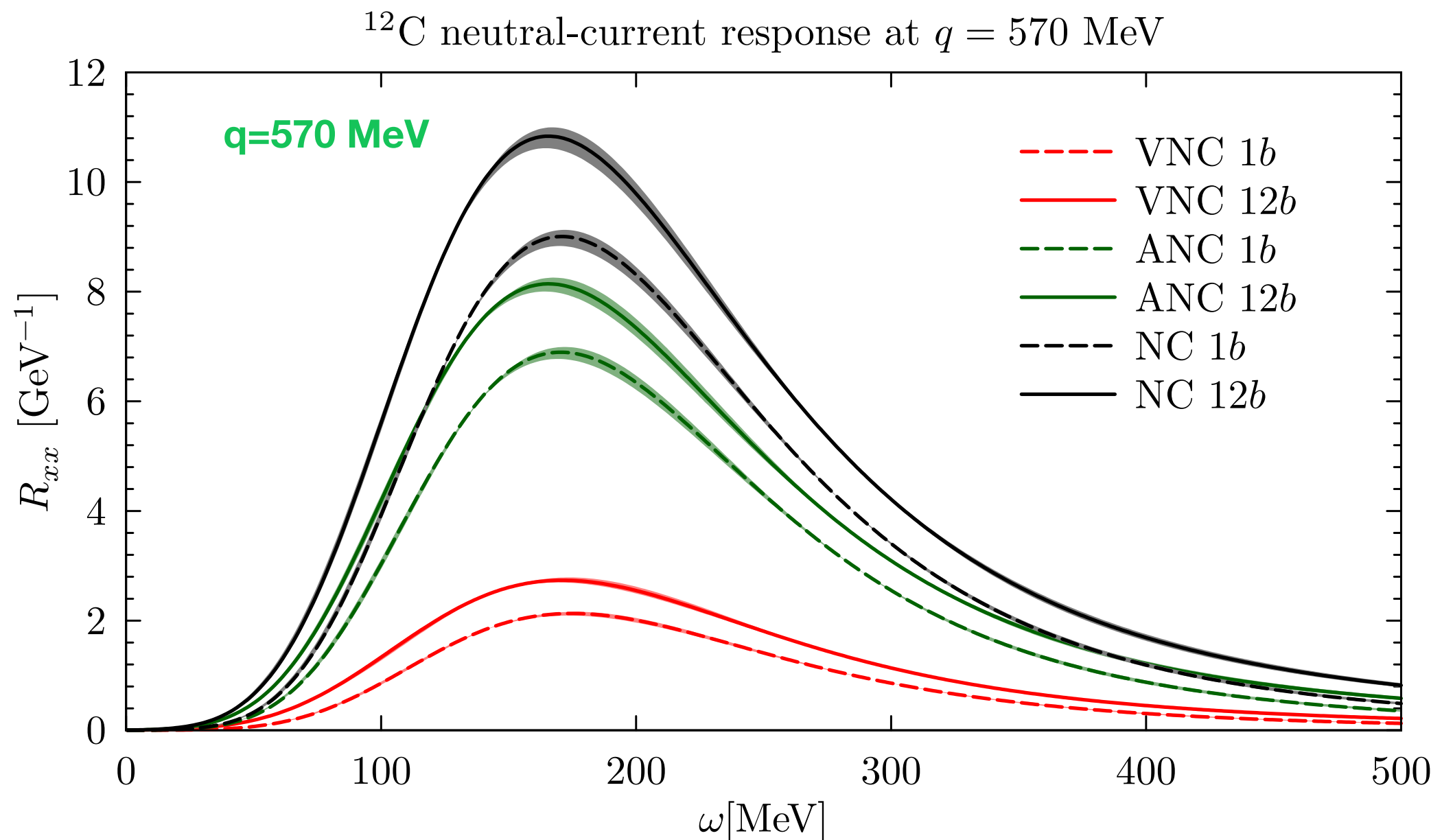
$$\rho_p(\mathbf{q}) = \sum_i e^{i\mathbf{q}\mathbf{r}_i} \frac{1 + \tau_{i,z}}{2} \quad \rho_N(\mathbf{q}) = \sum_i e^{i\mathbf{q}\mathbf{r}_i} = \rho_n + \rho_p$$



- In the impulse approximation the nucleon and the proton responses coincide
- GPMC results demonstrate the importance of the charge-exchange character of the nucleon-nucleon force

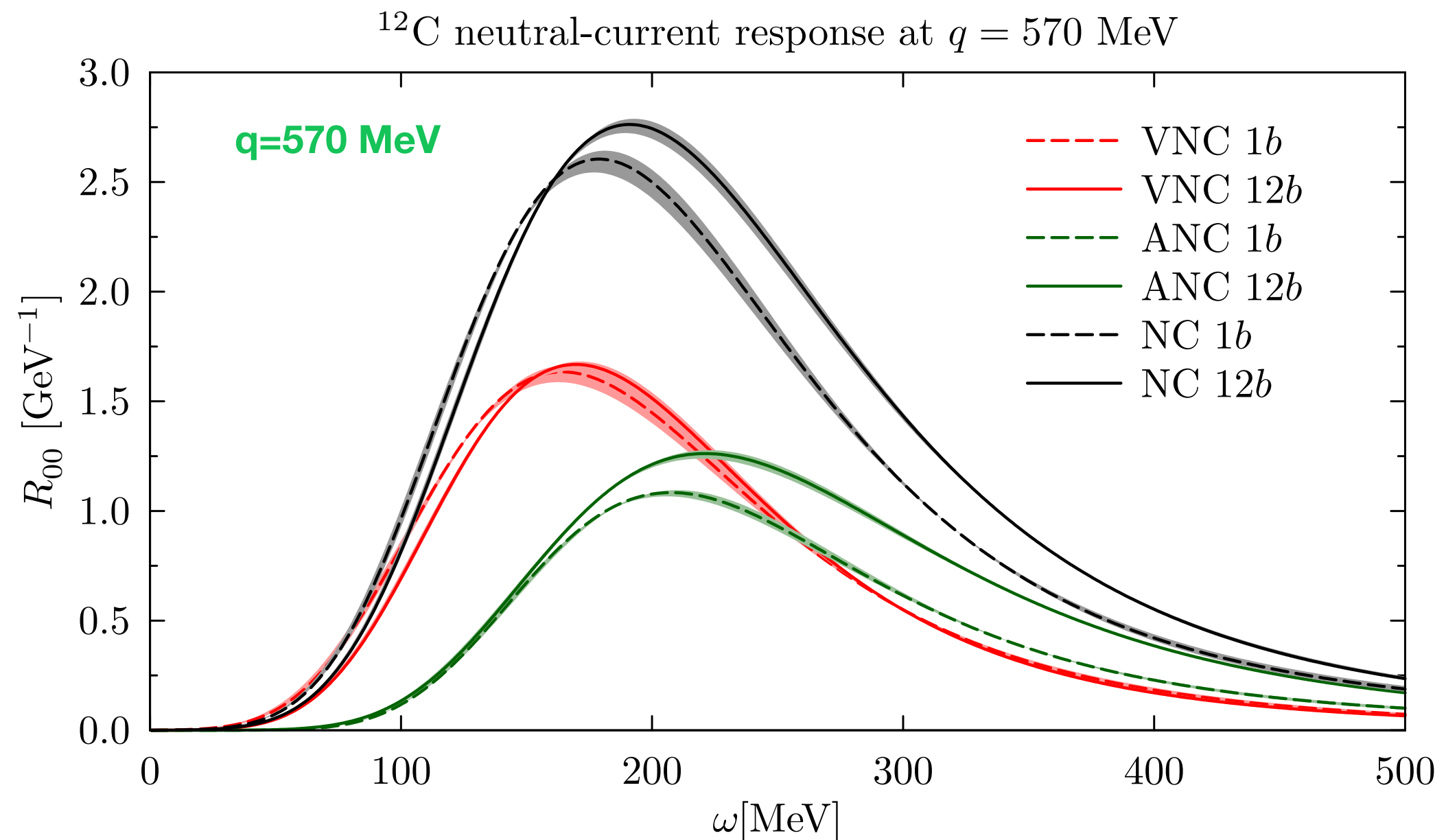
^{12}C neutral-current response

- Recently, we were able to invert the neutral-current Euclidean responses of ^{12}C



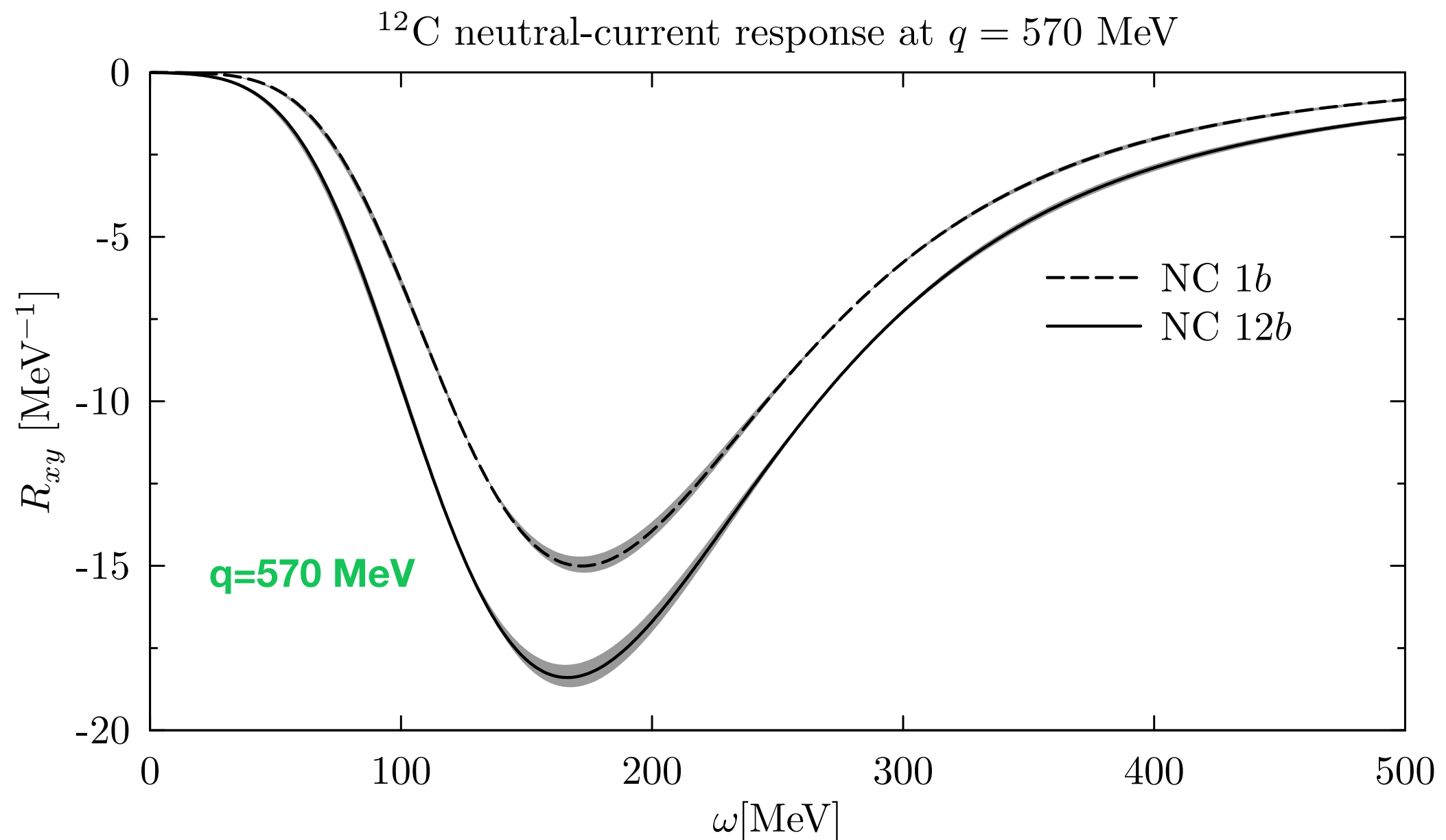
^{12}C neutral-current response

- Recently, we were able to invert the neutral-current Euclidean responses of ^{12}C



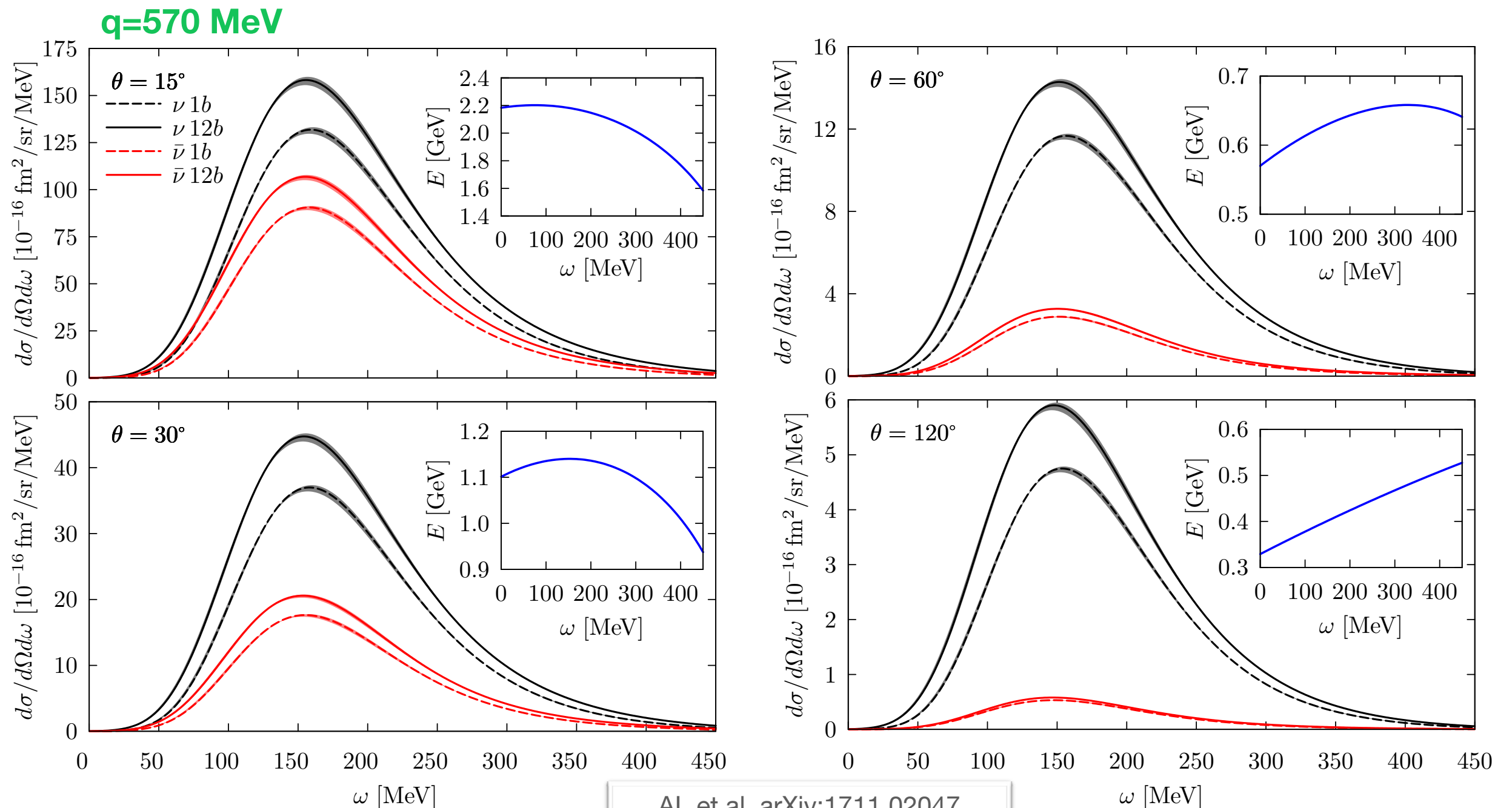
^{12}C neutral-current response

- We were recently able to invert the neutral-current Euclidean responses of ^{12}C



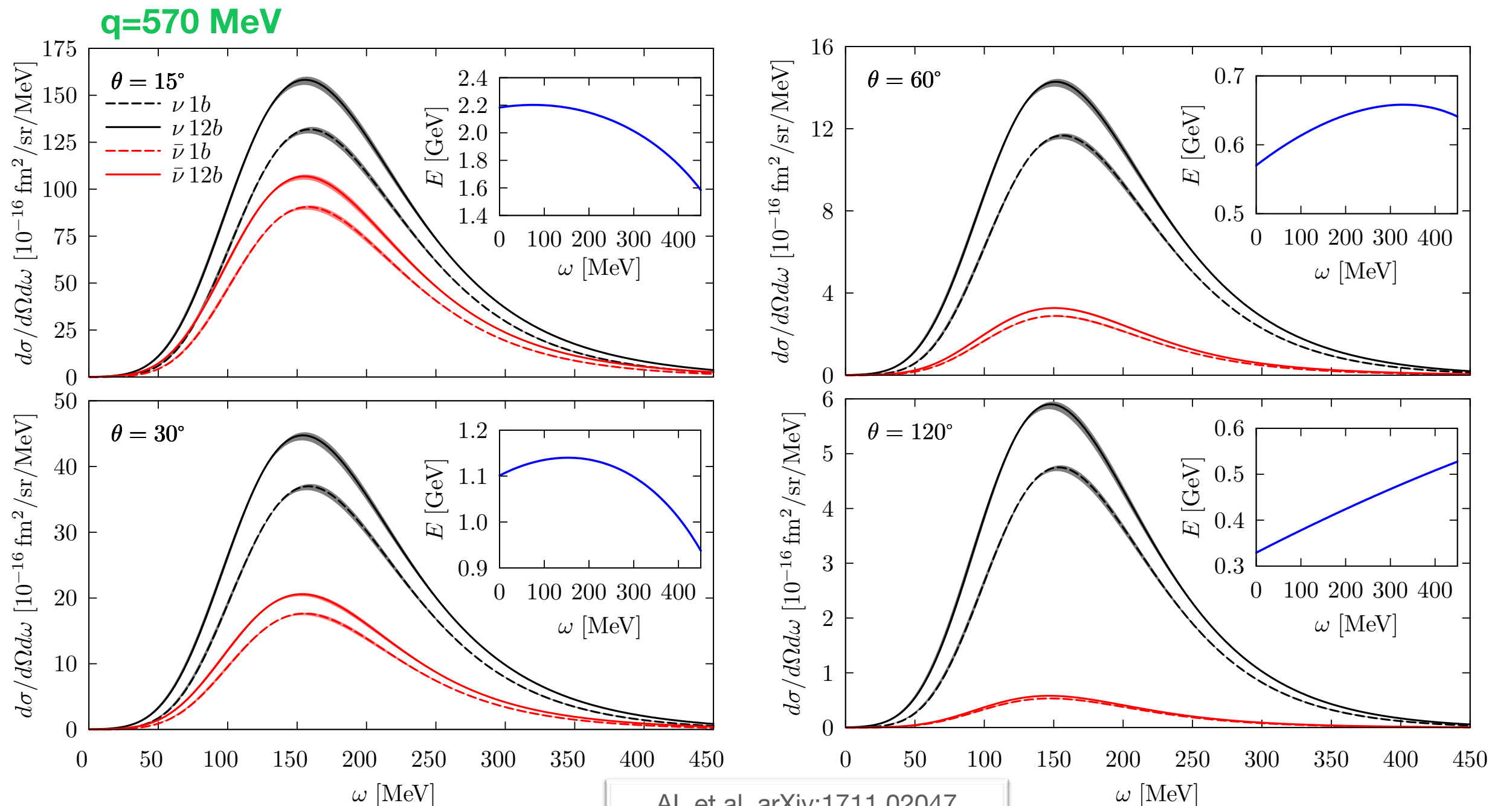
^{12}C neutral-current cross-section

- The anti-neutrino cross section decreases rapidly relative to the neutrino cross section as the scattering angle changes from the forward to the backward hemisphere



^{12}C neutral-current cross-section

- Two-body current contributions are smaller for the antineutrino than for the neutrino cross section, in fact becoming negligible for the antineutrino backward-angle



Relativistic effects in a correlated system

- Non relativistic approaches are limited to moderate momentum transfers
- In a generic reference frame the longitudinal non-relativistic response reads

$$R_L^{fr} = \sum_f \left| \langle \psi_i | \sum_j \rho_j(\mathbf{q}^{fr}, \omega^{fr}) | \psi_f \rangle \right|^2 \delta(E_f^{fr} - E_i^{fr} - \omega^{fr})$$
$$\delta(E_f^{fr} - E_i^{fr} - \omega^{fr}) \approx \delta[e_f^{fr} + (P_f^{fr})^2/(2M_T) - e_i^{fr} - (P_i^{fr})^2/(2M_T) - \omega^{fr}]$$

- The response in the LAB frame is given by the Lorentz transform

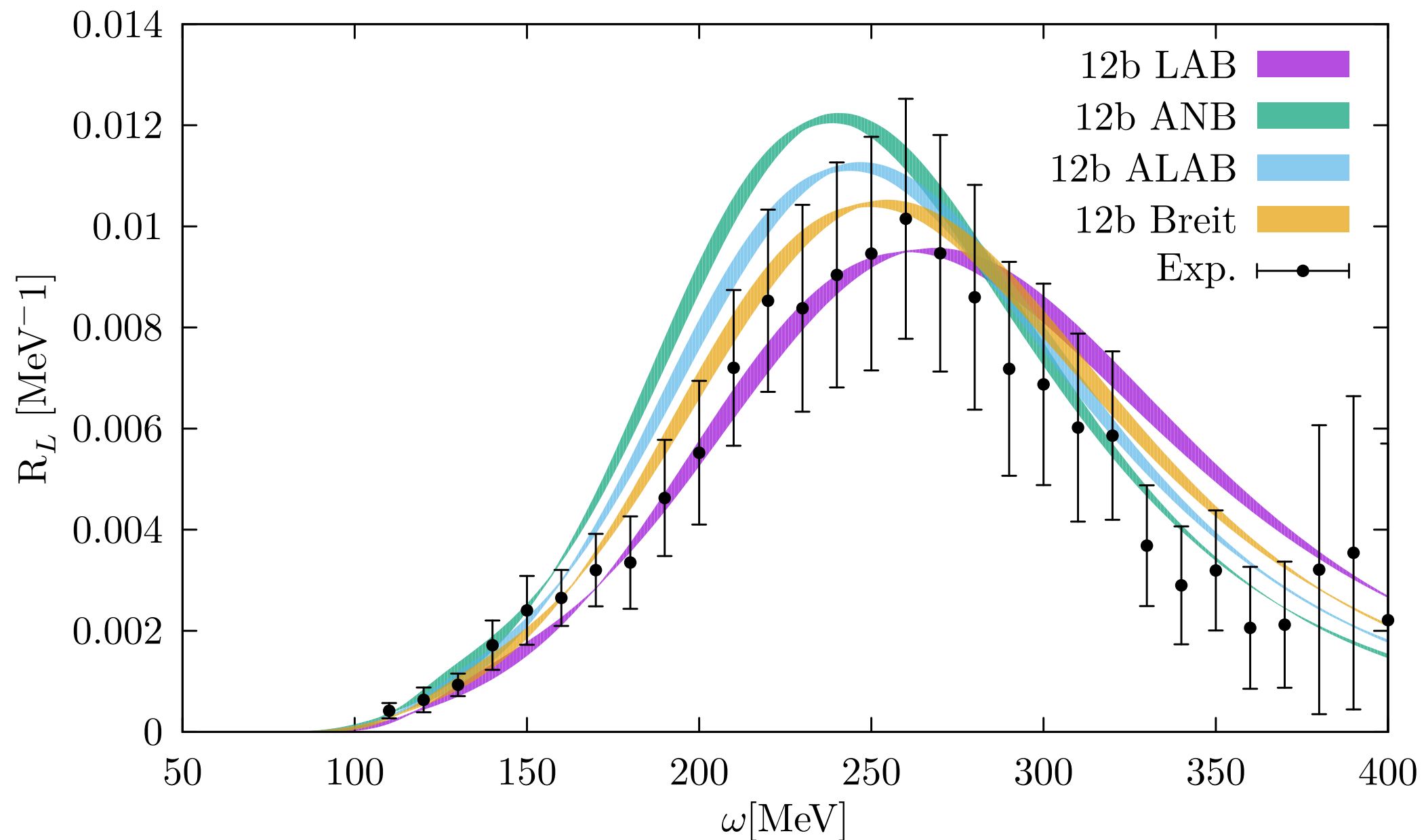
$$R_L(\mathbf{q}, \omega) = \frac{\mathbf{q}^2}{(\mathbf{q}^{fr})^2} \frac{E_i^{fr}}{M_0} R_L^{fr}(\mathbf{q}^{fr}, \omega^{fr})$$

where

$$q^{fr} = \gamma(q - \beta\omega), \quad \omega^{fr} = \gamma(\omega - \beta q), \quad P_i^{fr} = -\beta\gamma M_0, \quad E_i^{fr} = \gamma M_0$$

Relativistic effects in a correlated system

- The ^4He longitudinal response at $q=700$ MeV strongly depends upon the original reference frame



Relativistic effects in a correlated system

- To determine the relativistic corrections, we consider a two-body breakup model

$$\begin{aligned}
 p^{fr} &= \mu \left(\frac{p_N^{fr}}{m_N} - \frac{p_X^{fr}}{M_X} \right) \\
 P_f^{fr} &= p_N^{fr} + p_X^{fr}
 \end{aligned}
 \quad \longleftrightarrow \quad
 \mu = \frac{m_N M_X}{m_N + M_X}$$

- The relative momentum is derived in a relativistic fashion

$$\begin{aligned}
 \omega^{fr} &= E_f^{fr} - E_i^{fr} \\
 E_f^{fr} &= \sqrt{m_N^2 + [\mathbf{p}^{fr} + \mu/M_X \mathbf{P}_f^{fr}]^2} + \sqrt{M_X^2 + [\mathbf{p}^{fr} - \mu/m_N \mathbf{P}_f^{fr}]^2}
 \end{aligned}$$

- And it is used as input in the non relativistic kinetic energy

$$e_f^{fr} = (p^{fr})^2 / (2\mu)$$

- The energy-conserving delta function reads

$$\delta(E_f^{fr} - E_i^{fr} - \omega^{fr}) = \delta(F(e_f^{fr}) - \omega^{fr}) = \left(\frac{\partial F^{fr}}{\partial e_f^{fr}} \right)^{-1} \delta[e_f^{fr} - e_f^{rel}(q^{fr}, \omega^f)]$$

Relativistic effects in a correlated system

- The ^4He longitudinal response at $q=700$ MeV mildly depends upon the original reference frame

